

270
28-81
JW
MASTER

ENERGY

INDUSTRIAL ENERGY CONSERVATION



MASTER

Q.2274

2
February 6, 1981

NTIS-25
Birs - 162
State Government - 50

CONS-5089-11

PRODUCTION OF ALUMINUM-SILICON ALLOY AND FERROSILICON AND COMMERCIAL PURITY ALUMINUM BY THE DIRECT REDUCTION PROCESS

First Interim Technical Report, Phase C for January 1—March 31, 1980

By
M. J. Bruno

October 1980

Work Performed Under Contract No. AC01-77CS40079

Aluminum Company of America
Alcoa Laboratories
Alcoa Center, Pennsylvania

U. S. DEPARTMENT OF ENERGY

Division of Industrial Energy Conservation

DISTRIBUTION OF THIS DOCUMENT IS UNLIMITED

DISCLAIMER

This report was prepared as an account of work sponsored by an agency of the United States Government. Neither the United States Government nor any agency Thereof, nor any of their employees, makes any warranty, express or implied, or assumes any legal liability or responsibility for the accuracy, completeness, or usefulness of any information, apparatus, product, or process disclosed, or represents that its use would not infringe privately owned rights. Reference herein to any specific commercial product, process, or service by trade name, trademark, manufacturer, or otherwise does not necessarily constitute or imply its endorsement, recommendation, or favoring by the United States Government or any agency thereof. The views and opinions of authors expressed herein do not necessarily state or reflect those of the United States Government or any agency thereof.

DISCLAIMER

Portions of this document may be illegible in electronic image products. Images are produced from the best available original document.

DISCLAIMER

"This book was prepared as an account of work sponsored by an agency of the United States Government. Neither the United States Government nor any agency thereof, nor any of their employees, makes any warranty, express or implied, or assumes any legal liability or responsibility for the accuracy, completeness, or usefulness of any information, apparatus, product, or process disclosed, or represents that its use would not infringe privately owned rights. Reference herein to any specific commercial product, process, or service by trade name, trademark, manufacturer, or otherwise, does not necessarily constitute or imply its endorsement, recommendation, or favoring by the United States Government or any agency thereof. The views and opinions of authors expressed herein do not necessarily state or reflect those of the United States Government or any agency thereof."

This report has been reproduced directly from the best available copy.

Available from the National Technical Information Service, U. S. Department of Commerce, Springfield, Virginia 22161.

Price: Printed Copy A04
Microfiche A01

UNCLASSIFIED

PRODUCTION OF ALUMINUM-SILICON ALLOY AND FERROSILICON
AND COMMERCIAL PURITY ALUMINUM BY THE
DIRECT REDUCTION PROCESS

FIRST INTERIM TECHNICAL REPORT, PHASE "C"
FOR THE PERIOD 1980 JANUARY 01 - 1980 MARCH 31

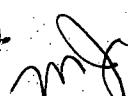
MARSHALL J. BRUNO

OCTOBER 1980

ALUMINUM COMPANY OF AMERICA
ALCOA LABORATORIES
ALCOA CENTER, PA 15069

PREPARED FOR THE
DEPARTMENT OF ENERGY
OFFICE OF THE ASSISTANT SECRETARY FOR
CONSERVATION AND SOLAR APPLICATIONS
DIVISION OF INDUSTRIAL ENERGY CONSERVATION
UNDER CONTRACT DEAC01-77CS40079

DISTRIBUTION OF THIS DOCUMENT IS UNLIMITED



THIS PAGE
WAS INTENTIONALLY
LEFT BLANK

FORWARD

This is the first interim technical report, Phase "C", submitted in accordance with the requirements of Contract No. DEAC01-77CS40079, a three-year cost-sharing agreement between the Department of Energy and Alcoa. The report describes work performed in the first quarter of the third year of the program.

TABLE OF CONTENTS

	<u>Page No.</u>
Abstract	1
Discussion	3
Progress	
A. Reduction - Phase C	5
B. Alloy Purification - Phase C	21
C. Purification to Commercial Grade Aluminum - Phase C	24
Phase C Second Quarter Program	28
Cost Summary	28
Assigned Personnel	29
Task/Milestone Schedule	29
 <u>List Of Tables</u>	
Reduction-	Tables 1 to 17
Alloy Purification-	Tables 18 to 21
 <u>List Of Figures</u>	
Reduction	Figures 1 to 6
Purification to Commercial Grade Aluminum	Figure 7
Appendix 1	FLWEQUIL AND FLWEQSEP Programs
Appendix 2	Carnegie-Mellon University Summary Report
	A-1
	A-3

Abstract

Phase C of a three year cost-sharing contract between the Department of Energy and Alcoa was started on 1980-01-01. At the end of the first quarter, the program for Phase C is estimated as 27.6% complete, with 28.3% of the funding expended.

Pilot reactor VSR-3 was operated with 75-120 SCFH O₂ to supply part of the process heat requirements by combustion of coke. No alloy was made and burden bridging persistently stopped operations. Burning larger coke particles, -3/8 in. +6 mesh, with O₂ injected through a larger diameter tuyere orifice resulted in oxygen attack on the reactor graphite liner. Updated thermochemical data for Al₂O significantly changed the calculated reflux loading for a one-atm blast furnace, predicting almost total reflux and no alloy recovery. Based on these calculations and the experimental problems with combustion heated operation, VSR-3 was modified to study an alternate reduction concept--the blast-arc--which utilizes combustion heat to reduce SiO₂ to SiC at 1600°C, and electrical heat to complete the reduction of Al₂O₃ and the production of alloy. The upper shaft of VSR-3 was tapered 14° from the vertical and the auger was replaced by a vertical stroke ram. A preheater was assembled to facilitate injection of 1800°C CO to the stage one reaction zone to simulate the effects of combustion products on the SiO₂ to SiC reaction. One run was made, yielding 33% alloy. The SOLGASMIX computer program was modified to treat ideal and non-ideal solution chemistry. Heat and material balances were calculated for three reduction processes, combustion, blast-arc, and electric. The electric process is most energy efficient, followed by the blast-arc, and the combustion process respectively. The bench scale reactor was operated to determine the effects of SiO₂/Al₂O₃ ratio, CO sweep and source of reduction carbon on alloy product yield. Starting up with substoichiometric carbon was beneficial to smooth operation, although steady state was not quite attained. SiO₂/Al₂O₃ ratio did not significantly affect metal yield at low CO sweep conditions. A series of alloy samples made in VSR-3 were remelted and analyzed in detail for phase identification by microscopic techniques.

Design, fabrication, and installation of most of the pilot crystallizer system was completed. The bench reactor was operated to determine the effects of copper additions

on alloy yield for impure alloy containing greater than 10% Fe. The technique did reduce the Fe level in the alloy product and increased yield. Leaching tests were also initiated to attempt to preferentially dissolve high Fe concentrations from alloy.

Fabrication and installation of the pilot membrane cell purifier components was continued. The control system was designed and instrumentation procurement was completed. The bench scale cell was operated to test graphite cements used in assembly of the pilot unit, different electrolyte compositions, and the resistance to metal penetration for the membrane cloth. A new bench unit was built to study polarization effects during electrolysis.

Primary activities in the second quarter of Phase C will include: beneficiation tests on high iron bauxites to reduce Fe and Ti; continued evaluation of the blast-arc concept in VSR-3; revision of VSR-3 to provide continuous tapping of metal product; development of flow sheets for a commercial blast-arc process; further evaluation of $\text{SiO}_2/\text{Al}_2\text{O}_3$ ratio and CO sweep in the bench reactor; determination of carbon solubility in Al-Si alloys; completion of pilot crystallizer installation and start-up for shake-down; continuation of pilot membrane cell installation.

Discussion

The primary objective of the three-year program is to demonstrate technical feasibility of a pilot sized Direct Reduction Process for producing aluminum and aluminum-silicon alloy. The process includes three major tasks, Reduction to produce impure alloy, Alloy Purification and Purification to Commercial Grade Aluminum. Goals for the third phase are to determine the feasibility of supplying high temperature reaction heat by oxygen combustion of coke in the vertical shaft reactor, to evaluate alternative reduction processes utilizing electric heat in the metal-producing zone, to complete construction and installation of the purification pilot units, and to demonstrate alloy refining and purification in the pilot units.

In the first quarter of Phase C, the following work was accomplished by subcontractors and consultants. Koppers Company submitted a list of recommendations relating to agglomeration of burden materials and supplied information on Reichardt diagrams for the staged process heat balance calculations. Carnegie-Mellon University completed a series of experiments on the effects of SiC and Al_4C_3 on vapor losses. Aluminum vapor losses were high regardless of the SiC or Al_4C_3 levels employed. Details are given in the Appendix. Professor J. Szekely consulted a total of 6.5 days on heat and material balances and computer modeling. Dr. J.C. Agarwal, Charles River Associates, Inc. consulted for 5 days on reduction process flow concepts and process economics.

A technical paper "Computer Aided Model of Coke Fired Reduction of Alumina-Silica" was presented at the annual AIME meeting by N.M. Fitzgerald of Alcoa. Also, a technical article, "Method of Carbothermically Producing Aluminum-Silicon Alloy" by C.N. Cochran, Alcoa, was published in the March 1980 issue of Aluminium.

The Department of Energy approved a subcontract for Charles River Associates, Inc. Approval was also granted to proceed with Phase C of the contract.

Alcoa requested a contract modification for DOE to revise Phase C sub-tasks, reducing the effort on the Alloy Purification and Purification to Commercial Grade Aluminum tasks. The level of effort on the Reduction task will be maintained at a high rate.

The status of the project was reviewed with the DOE project manager and Professor J.F. Elliott once during this quarter. Also, a presentation of the Direct Reduction Process including current status was made for Mr. J. Dodd, Office of Management Budget.

Progress for the three main tasks is reported by sub-task as identified in the modified task descriptions submitted on 1980 March 26. It is estimated that for Phase C, the Reduction task is 26% complete, the Alloy Purification task is 42% complete, and the Purification to Commercial Grade Aluminum task is 27% complete at the end of the first quarter.

PROGRESS

A. REDUCTION - PHASE C

Task No. 1: Supply Burden Material

Table 1 lists the burdens prepared in the first quarter of Phase C. Burden materials having 80% stoichiometric reducing carbon and $\text{SiO}_2/\text{Al}_2\text{O}_3$ ratios of 0.5, 0.788, and 1.0 were prepared from -200 mesh Tyler feedstocks of bauxite, kaolinite clay, and COED char in the Eirich mixer. The sized product yield of 3.35 by 1.70 mm (6 x 10 mesh Tyler) were 55% and 45% respectively for $\text{SiO}_2/\text{Al}_2\text{O}_3$ ratio of 0.5 and 1.0. The average fired (1000°C) compressive strengths for 3.2 mm (0.125 in) dia balls were 1.49 MPa (217 lb/in²) and 2.05 MPa (298 lb/in²) and were a function of the kaolinite contents of these mixtures. The 0.5 and 1.0 $\text{SiO}_2/\text{Al}_2\text{O}_3$ ratio mixture contained 39% and 64% kaolinite respectively.

Eirich mixer balls having an 0.788 $\text{SiO}_2/\text{Al}_2\text{O}_3$ ratio and 55% kaolinite were prepared to give a 9.5 by 3.35 mm (0.375 by 0.132 in) product. The yield of 9.5 by 3.35 mm product was 64%. The average fired (1000°C) compressive strength of 3.2 mm dia and 6.3 mm dia balls was 2.80 MPa and 0.96 MPa (406 and 139 lb/in²) respectively. The high compressive strength of the 3.2 mm dia balls is due to the coarser particle size distribution of this material (9.5 x 3.35 mm) compared to the finer particle size (3.35 x 1.70 mm) of the other two mixtures.

Task completion is 25%.

Task No. 2: Burden Beneficiation

No Progress.

Task completion is 0%.

Task No. 3: Effects of Pilot Operating Parameters

In January, four runs were conducted in an attempt to make metal while burning coke and oxygen. The details of these runs are shown in Tables 2 and 3. Two of these runs were terminated due to an auger shear pin failure, one run due to bridging below the auger, and one due to severe bridging

in the auger. No alloy was produced. During these runs, the oxygen rate was systematically lowered from 120 CFH to 75 CFH to decrease the CO sweep and vapor species recycle and enhance metal production. In the final run, VSR-3-31, the auger was finally located at a proper depth in the bed to break up the bridge as it was formed. It appeared that the bed in the auger remained open although buildup occurred on the bottom of the auger blades in the heavy bridging area. However, the annular space between the auger and the furnace wall plugged, restricting the downward motion of the bed. A higher auger rotational speed may result in less plugging of the bed in the bridging zone in any future runs.

It had been previously determined from VSR-3-21 that larger heating coke might result in less carbiding of the metal. The coke size was therefore increased to -3/8-in. +6 mesh for VSR-3-28 through VSR-3-30. Based on the assumption that the tuyere orifice diameter should not be smaller than the largest coke particle for the establishment of a proper raceway and the attendant control over the combustion process in a blast furnace, the tuyere diameter was increased to .4-in. I.D. Unfortunately, this desire to use larger coke was at odds with attempts to decrease the oxygen rate and the attendant CO sweep such that there was severe oxidation of the carbon liner around the tuyeres in VSR-3-30. In VSR-3-31, coke size was returned to -1/4-in. +6 mesh. The 1/8-in. to 3/8-in. tapered nozzle tuyeres were again used. The total O_2 flow was decreased to 75 CFH for that run, but again there was severe O_2 attack around the tuyeres. In any future heating coke runs at low O_2 , it may be necessary to use a tuyere of a smaller diameter than the coke particle size to prevent the burning of the furnace walls.

Recent thermodynamic equilibrium calculations (see Task No. 5) reflecting an update of Al_2O suboxide Gibbs Free Energy data have indicated a much larger reflux requirement for the operation of a fully combustion heated carbothermic Al-Si process than was previously expected. These calculations show that at one-atmosphere total pressure the recycle of metal species is 100% indicating no metal production, but that some yield can be expected at three atmospheres. Based on this three-atmosphere case for a .518 SiO_2/Al_2O_3 weight ratio, 1.217 gm total charge/gm O_2 are required to make the energy and mass balance. This case is compared to the more recent pilot reactor combustion runs in Table 2 to show that in all runs, except for VSR 30 and 31, CO sweep from combustion was excessive.

The oxygen rates for VSR-30 and 31 were respectively only 70% and 80% of that required for the three-atmosphere case. Still, it is unlikely that metal would be produced at one atmosphere for these rates.

A series of experiments was conducted to determine if oxygen is present across the entire cross-section of the pilot reactor at the tuyere level. Al-Si alloy formed above the centerline of the tuyeres may be reoxidizing in the presence of unreacted O_2 , and a method for directing metal past the tuyeres at low oxygen potential had to be found.

Graphite rods (3/16-in. O.D.) were therefore imbedded in the grate during runs 32 and 33 to detect the presence of oxygen in the radial direction across the reactor. These graphite rods extended approximately 4-in. above the centerline of the tuyeres. Pure oxygen at 60 SCFH was injected through one tuyere during VSR-32 and 33 after the vessel was brought to temperature by induction heating. The progress of the reactions prior to O_2 combustion was followed by monitoring the concentration of carbon monoxide in the off gas. A single 3-in. layer of ore was placed between upper and lower coke beds to study the migration of ore constituents throughout the reactor.

Although both runs were discontinued due to bridge formation in the shaft, the burning profile of the graphite rods revealed that the blast was not penetrating across to the opposite wall. This implied that reduced constituents (metal) could pass the tuyere region at the wall opposite to a single O_2 injection tuyere in the pilot reactor without being reoxidized.

A re-evaluation of the thermodynamic equilibrium for producing Al-Si alloy at one atmosphere in the presence of CO sweep has recently been performed. The yield of alloy for even modest levels of CO produced by coke-oxygen combustion in the Stage II and III metal producing zones is minimal. If adequate carbon (coke) is charged to the reactor to meet the total energy requirement for the process by coke-oxygen combustion, the one pass yield of Al-Si alloy entering the hearth region is less than 5%.

Therefore, pilot reactor testing in March was redirected toward investigating the feasibility of operating an alternative combined "blast-arc" technique for producing metal. In this arrangement 40 to 60% of the energy of the process would be supplied by combustion in the upper stack to convert silica (SiO_2) to silicon carbide (SiC). Coke in the bed

could be combusted by means of oxygen injection into the stack or a series of char(or coal)-oxygen burners could be placed around the circumference of the reactor. Silicon carbide would be produced at bed temperatures between 1550 to 1850°C by the reductant carbon contained in the bauxite-clay-coke pellets in an atmosphere of combustion products (primarily CO) and ascending volatile species. In the lower section of the shaft Al-Si alloy would be produced by means of energy from an electric arc or induction system. Silicon carbide formed in the stack and unreacted carbon in the pellets would complete the reduction of Al_2O_3 at 2125°C to the metallic Al-Si phase.

In order to commence demonstration of the "blast-arc" concept, the pilot reactor was modified during March to inject pre-heated carbon monoxide at approximately 1850°C into the Stage I region to simulate the effects of combustion products on the formation of SiC. A schematic of the redesigned reactor is illustrated in Figure 1 and is described under Task 4.

The initial experimental run (VSR-35) with this modified-design reactor was made during March. Prior to injecting CO through the inner tube, the reactor was brought to temperature by means of the induction system and bed movement corresponded to a charging rate of 4 kg of ore/hr. At this time, a bridge formed at the elevation of the CO injection tube and the auger snapped at the connecting tube.

The run, however, was continued for 30 minutes to check the CO injection system. Carbon monoxide (150 SCFH) was successfully preheated to 300°C in the external packed bed and was passed upward through the reactor. Based on the temperature of the tube in the internal packed bed (obtained by sighting through the bottom glass prism) and heat transfer calculations, the CO gas was successfully heated to 1850°C at the point of injection.

An autopsy of the reactor revealed a 4.1 kg ingot of Al-Si alloy in the catchbasin. Since 11.9 kg of ore had been charged to the shaft during the run, a yield of 33% (kg of ingot/kg of charged ore) was obtained. Surprisingly, this yield corresponds to the theoretical steady-state yield of alloy from raw ore. Carbon monoxide evolution from the reacting ore was considerable during the run and exceeded four moles of CO/mole of Al in the ingot.

Task completion is 25%.

Task No. 4: Pilot Modifications

Carbon monoxide which has been preheated by an external bed to 300°C is being passed upward through the reactor into an internal bed of graphite particles (.75-in. O.D., .50-in. I.D., .25-in. Wide). As confirmed by heat transfer calculations, these graphite particles which are irradiated by the bottom induction coil will heat as much as 300 SCFH of CO to 1800°C. The CO will then be injected at a point in the reactor shaft where the temperature of the gas approaches the temperature of the solid bed.

To remedy the bridging phenomena, the upper geometry of the shaft was altered in an attempt to reduce the tendency for bridging of molten material. Figure 1 illustrates a tapering of the reactor susceptor to an angle of 86° similar to the stack batter on a commercial blast furnace. Hopefully, the divergence of material in the lower taper section with the assistance of a reduced diameter auger or vertical stroke "ram" (not shown) will prevent future bridging problems.

Task completion is 25%.

Task No. 5: Reactor Scale-Up Design

A series of heat-up and steady-state temperature profiles were computed for a proposed 16-in. dia pilot reactor with an external, induction heating system. Results indicated that heat-up to approximately 2200°C required about two hrs at full power or four hrs at 50% power, when full power was 175 KW. Steady-state profiles predicted bed wall to bed center temperature differences of about 100°C. Heat losses through the reactor shell over a vertical length of 1.98 m was calculated as 21.2 KW. Time-temperature and temperature-distance (fraction of radius) curves are shown in Figures 2-5.

Task completion is 15%.

Task No. 6: Calculate Heat and Mass Balance

The SOLGASMIX computer program for calculation of chemical equilibria was modified to treat ideal and non-ideal solution chemistry, facilitating consideration of solutions in the products. SOLGASMIX is the equilibrium calculator used in all of the computer programs, FLOW REAC, FLWEQUIP, and FLWEQSEP.

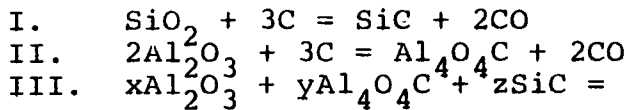
Heat and materials balances were calculated for three reduction processes, electric, hybrid, and combustion, and a Reichardt diagram was constructed for the latter case. Using corrected data for $\text{Al}_2\text{O}_4\text{C}$ and Al_2O , it was found that a one-atmosphere combustion heated process will have insignificant one-pass yield (~100% recycle ratio), while a three-atmosphere process will have a one-pass yield ranging from 0-25% depending upon the assumed activity of aluminum and silicon in the alloy. Further work is necessary to make the best estimate of activities. When calculated on a common basis of 1 g Al made by refining and purifying an Al_3Si_2 alloy diluted by typical amounts of Ti, Fe, and C, the net energy requirements for the electric, hybrid, and combustion processes were calculated to be 109.7, 126.3, and 253.5 KJ/gAl. This is a complete reversal of the initial estimates for these processes. A scheme for computing the Stage III equilibrium using a programmable calculator was used to study the effect of changes in heats of formation and activities.

A thermochemical model of the carbothermic reduction of Al_2O_3 , SiO_2 , and C to an Al-Si alloy initially gave results which suggested that the reduction process might be feasible in a combustion-heated shaft furnace similar to an iron blast furnace. Based on the model, the net energy requirement on a coal basis was calculated to be substantially less than the Bayer-Hall process, provided credits could be taken for CO and ferrosilicon. Two other carbothermic reduction processes, the electric arc and the blast-arc, also were calculated to have a substantially lower energy requirement on the same basis. Review of the early modeling work revealed four problems.

1. The $\text{Al}_2\text{O}_4\text{C}$ data was incorrectly entered into the computer data base.
2. The Al_2O data was based on 1972 JANAF data. This data was revised in the 1975 JANAF supplement resulting in a change in the Gibbs free energy of formation of about -4000 cal/mole.
3. The activities for Al and Si in the computer data base were based on Russian data measured at 1700°C, and extrapolated to higher temperatures based on constant excess entropy. Later Russian data indicated that the alloy became more ideal at higher temperatures.

4. The heat balance for the three-atmosphere blast furnace process did not quite balance due to a deficiency of high temperature heat.

The carbothermic reduction process can be separated into three main reaction stages assumed to occur in a shaft reactor with primary heat input at the bottom.



These reactions are incomplete as written since the volatile species, Al, Al_2O , and SiO are not considered. The Stage III reaction has the flexibility to produce an alloy where composition ranges from approximately Al_3Si_2 to Al_2Si_3 . In the following calculations, the computer considers the alloys to be a series of compounds, Al_xSi_y , where $x + y = 10$. Ti, Fe, and C in solution are not considered nor are the possibilities of an oxycarbide ($\text{Al}-\text{O}-\text{C}$) "slag" solution or alloy solution with continuously variable composition.

Table 4 is the materials balance by stages. The one-pass aluminum yield, defined as the aluminum leaving as alloy divided by the aluminum in the $\text{Al}_4\text{O}_4\text{C}$ assumed to recycle. In Table 5, the complete heat balance by stages is presented. Since the thermal mass ratio* is about 0.5, the CO is assumed to be cooled to the entering solids temperature. The total heat requirement for the electric process is 3909 kJ/mol Al_3Si_2 . This value could be lowered slightly by taking credit for the condensation of SiO from Stage I.

The hybrid process is assumed to be electrically heated in Stages II and III, and combustion heated in Stage I and the preheat zone. It is assumed that C and O_2 are combusted adiabatically and supply heat at 1840°K, the temperature of Stage I. The heat balances for Stages II and III are identical in the electric and hybrid cases. The hybrid Stage I was recalculated with ARLEQUIL to determine the effect of the additional CO sweep on the heat requirement due to additional SiO formation. Table 6 shows the complete heat balance by stages for the hybrid process. The enthalpy of the gas is greater than that of the solids, so the gas

*Reichardt ratio = $C_{pg}G_g/C_{ps}G_s$ where C_p is specific heat, G is mass flow rate.

exists at an elevated temperature. The hybrid process requires 2461 KJ/mol Al_3Si of electric heat and 19.9 mols of C to supply the combustion heat. This represents a 37% reduction in electrical heat requirements.

The combustion heated process was separated into five stages by including a mullite formation stage and separate stages for SiC formation from mullite and excess silica. In order to be consistent with previous reports, Stage III was initially computed for reduction of Al_2O_4 by SiC. An initial run indicated that the one-pass aluminum yield for a combustion heated process was nearly zero at one-atmosphere pressure. The pressure was then increased to three atmospheres for all the stages and significant one-pass yield was found, although the alloy composition shifted to $Al_3Si_1.29$. Table 7 shows a staged materials balance. A Reichardt diagram was constructed (Figure 6). This diagram is a plot of enthalpy transferred from the gas to the solid as a function of temperature. The significance of the diagram is threefold:

1. The "pinch point" occurs in Stage III so the process is controlled by high temperature heat input. This simplifies the analysis of the process since the Stage III heat balance will define the energy requirements.
2. Condensation of Al, Al_2O , and SiO releases sufficient heat to carry out Stages II, Ib, and part of Ia as well as raising the temperature of the solids between Stages II and Ia.
3. The thermal mass ratio is relatively high, so the solids would be rapidly heated to Stage I while the gas will exit at a temperature close to 1000°C.

The case presented here was slightly deficient in high temperature heat so the O_2 was assumed to be preheated to 630°K. The one-pass aluminum yield for Stage III was 38.9% which means 61.1% of the aluminum was volatized and assumed to recycle. A more realistic case was run with 25% more combustion heat. The one-pass aluminum yield for Stage III dropped to 33.9%. Carbon consumption rose from 49.73 to 60.38 moles/mole $Al_3Si_1.29$.

In order to compare the combustion heated processes to the electric and the hybrid processes, Stage III was recalculated with the addition of Al_2O_3 in order to make Al_3Si_2 .

Combustion heat input was increased by 10% over that required to balance Stage III. The one-pass aluminum yield decreased to 25.2% while the carbon consumption rose to 84.64 moles/mole Al_3Si_2 .

The heat and material balances discussed above were used as the basis for a comparison of the energy requirements for the three thermal processes. Table 8 shows an analysis of an ore typical of the bauxite-clay-coke pellets now being used in experiments. The analysis was normalized to exclude minor constituents. The table also shows a materials balance for the by-products likely to be recovered if the alloy is refined and purified to Al. Metallographic examination indicated that FeSiAl_5 , SiC , and TiSi_2 are present in samples of ingots although FeSi_2Al_4 and Al_4SiC_4 may be present. Some solubility of Al and Fe in TiSi_2 has been detected with a microprobe. The composition of the alloy as tapped is roughly Al_3Si_2 diluted by Ti, Fe, and C.

Assumptions used in these calculations are listed below.

1. Electricity is obtained from a mixture of 86% fossil and 14% hydro resulting in an efficiency of 42.5%. Electrical energy is divided by .425 in order to obtain total energy.
2. The total energy value of C based on combustion to CO_2 is 32.79 KJ/gC. Combustion of CO to CO_2 has a credit value of 23.59 KJ/gC.
3. Alloy refining uses 2.4 KJ/g alloy \times 1.16 g alloy/gAl of electricity.
4. Aluminum purification was 18.6 KJ/gAl of electricity.
5. The O_2 plant requires 1.32 KJ/g O_2 of electricity.
6. Carbon is assumed to be coke carbon which is produced from coal carbon at 80% efficiency.

Several other assumptions were also used.

1. Credit for metalloid by-products (SiC , FeSiAl_5 , TiSi_2 , Si) is based on the electrical energy value of the heats of formation of the highest oxides plus the carbon energy value of the carbon for reduction. This is shown in Table 9.

2. Calcination of ore pellets requires 10.1 KJ/gAl based on heating the pellets to 1000°C and evaporating the water of hydration. This is assumed to be electric energy for simplicity.

3. Reduction of TiO_2 and Fe_2O_3 plus the possible heat of Fe , Ti , and C requires 2.3 KJ/gAl. This is assumed to be electric energy for simplicity.

4. Heat losses are assumed to be 10% each for electric heat and for combustion heat above the critical temperature, 1840°K for the hybrid process and 2400°K for the three atmosphere combustion process.

Table 10 shows the calculations of the electric and coal energy requirements and the CO and metalloid by-product credits for the three processes. In Table 11, three variations of the electric and hybrid processes are compared with the combustion process. The variations are: coke as the solid fuel and reductant at 80% efficiency, coal as the solid fuel and reductant at 100% efficiency; coal with electricity generated by combustion of CO at a 35% efficiency.

The significant feature of these calculations is that the relative positions of the three thermal processes with respect to energy efficiency are reversed from the initial calculations. The arc is more efficient than before because a 10% rather than a 28% heat loss is assumed. The higher heat loss was based on a pilot arc furnace. The combustion process is much worse than before because the higher volatility of Al_2O and the higher CO sweep required to supply the 10% heat loss above the critical temperature. The high recycle ratio greatly increases the high temperature heat requirement. The most efficient process is the electric process using coal as a reductant. If minimal purchased electricity energy is desired, the hybrid process using coal is most efficient since the electrical energy requirements can be substantially reduced by burning CO to generate electricity. The electric and hybrid processes are generally more than twice as efficient as the present Bayer-Hall process.

In order to check the sensitivity of the thermochemical calculations to changes in free energy of formation and activities of various constituents, a set of equations was constructed to represent Stage III equilibrium. These

equations are shown in Table 12. Equilibrium constants as a function of temperature were used to calculate the partial pressures of CO, Al, Al_2O , and SiO . Using a programmable calculator, temperature was varied by trial and error until the sum of the partial pressures was equal to the desired total pressure. Using the relationship between the various species in the four chemical equations, mass balances were used to calculate the amount of aluminum and silicon in the solid, liquid, and gas phases. One-pass yields for aluminum and silicon, defined as the number of moles in the liquid divided by the total number of moles reacted, was then calculated.

Table 13 presents the calculated partial pressures, reaction temperature, and one-pass yields for two values of G_{fAl_2O} and three values of activities. For an ideal solution, G_{fAl_2O} changes from .0638 to .1338 when the 1972 JANAF data for Al_2O is replaced by the 1975 data. The aluminum losses to the gas phase ($100\% - Y_{Al}$) increased by 75%. When activities for an ideal solution were substituted for values determined experimentally at $1700^{\circ}C$, the aluminum losses to the gas phase increased by 130%. Meaningful modeling of this system will require estimates of activities in which some confidence can be placed.

Comparison of the calculated partial pressures, temperature, and yields with those computed by SOLGASMIX show fairly good agreement for aluminum, but only fair agreement for silicon. These calculations are still being reviewed.

Task completion is 30%.

Task No. 7: Process Mathematical Modeling

The FLOW REAC computer program for steady-state calculations was updated in the areas of reaction rate expression input, reaction heat assignment, treatment of external heat input or loss, and assignment of temperature limits.

The kinetics computer model reported under Task 2 of Phase B was simplified, eliminating the uncertainties involved in modeling kinetics parameters and adapting it to calculation of equilibrium heat and mass transfer. Two versions of the chemical equilibrium/heat transfer model were developed, FLWEQUIL and FLWEQSEP, differing in their handling of backward-flowing phases. A more detailed description of these programs is given in Appendix 1.

Task completion is 50%.

Task No. 8: Effects of Process Variables

Nine runs were made in the bench reactor in this quarter. The first run, AF-7, which was a successful induction run with no CO sweep, duplicated the conditions of VSR-3-19, the most successful pilot plant induction run to date. Runs AF-8 through AF-11 were attempts to operate the bench-scale reactor in a continuous mode while passing 15 liters/minute of CO sweep through the entire bed. With some experimental changes, runs AF-12 through AF-15 were successfully operated at the same 15 liters/minute of CO sweep. The main variables in these runs were the $\text{SiO}_2/\text{Al}_2\text{O}_3$ ratio and the source of reduction carbon in the ore burden.

Basically, only the position of the induction coil was varied during the first four CO sweep runs. The intention was to decrease the axial temperature gradient in the back-reaction or bridging zone to prevent a concentration of these reactions over too small a volume. It was believed that by forcing the back-reactions to be distributed over a long zone, less severe bridging would occur and a continuous operation could be obtained. Sufficient carbon for 100% reduction of oxides was charged in the first five runs and in all cases large accumulations of residue containing mostly carbide were found on top of the grate extending up to the bottom of the auger. Also, the temperature in the susceptor at the bottom of the auger was above 1900°C and often evidence of liquid material could be found on top of the carbide accumulations at the bottom of the auger. One other observation was that the bulk density of carbides was so low that their formation quickly consumed a large volume of the furnace. A possible explanation of these phenomena is as follows.

Initially, the suboxide vapors leave the metal-producing zone resulting in accumulations of unconsumed reduction carbon from the burden and the metal formed easily carbided. As these back-reacted suboxides recycle to the metal-producing zone, the accumulated carbides are consumed by the excess oxides that would accompany the downcoming burden. It appeared, however, that as the carbides formed and filled up the bottom of the furnace, the metal-producing zone was raised to higher levels until these endothermic reactions were either quenched on the bottom of the auger, which acts as a heatsink, or was raised out of the temperature region

which was sufficiently hot enough to make metal. The proper strategy appeared to be to start out with a sub-stoichiometric burden then gradually charge a higher carbon burden to prevent the accumulation of too much oxide slag in the metal-producing zone. Since the internal furnace hardware and auger are made of graphite and some oxide dust can be found in the off-gas, the ore must contain less than 100% stoichiometric carbon.

In AF-12 through AF-15, the burden contained only 80% of the reduction carbon requirement and the bottom of the auger was kept cooler by compressing the induction coil into the high temperature metal-producing region. As a result, each run was stopped only after the reservoir was full of metal. Each of these runs had an accumulation of slag on top of the grate and minor amounts dripped through the grate to the reservoir below. The first metal formed poorly coalesced in the bottom of the reservoir and the ingot structures were very heterogenous and difficult to characterize as to the composition and constituents of the continuous phase of operation. However, the ingot structure generally had a zone of metal with high concentrations of carbide, intermetallic, and slag on top of the poorly coalesced metal with a purer metal component near the top of the ingot. The slag may be denser than the metal since it was always found below the metal surface.

Phase analysis by metallography (see Table 14) and x-ray diffraction both indicate that Al_4SiC_4 is found in the metal phase for $\text{SiO}_2/\text{Al}_2\text{O}_3$ ratios in the burden of .6 and .5 but not for ratios of .78 and .99. Increases of SiO_2 in the ore did not necessarily result in increases in the hypereutectic Si phase. The first metal formed solidified as uncoalesced droplets with a skin of SiC at the surface and a typical solidification pattern of metal rich in slag, carbide, and intermetallics at the bottom of the droplet and purer metal near the top. This tendency for non-coalescence increased as the ore $\text{SiO}_2/\text{Al}_2\text{O}_3$ ratio decreased. The slag content of the ingot increased with increasing $\text{SiO}_2/\text{Al}_2\text{O}_3$ ratio. No definitive slag layer was found in the ingots for AF-7 and AF-13. Possibly slags in lower Al_2O_3 systems are less viscous.

The analysis of the first and last metal to form is compared to ore composition in Table 15. It does not appear from these analyses that a steady-state was reached in any of these runs as the incoming ore Si/Al ratio did not equal that of the metal product. However, each run appeared to approach a steady-state from the lower side as the top metal Si/Al ratio was higher than that of the first metal and more

closely approached the ratio for the ore. These analyses also indicate that Si is accumulated in the furnace either as SiC or recycled SiO more preferentially than Al. It is very difficult to draw any conclusions from the carbon analysis, the SiC phase analysis in Table 14, and the fact that higher Si metal coalesces better than lower Si metal. Characterization of Al-Si-C liquid alloys in the presence of C and SiC solids is necessary to understand these results. Attempts will be made at a characterization of this system in sufficient detail to explain our bench-scale results.

A comparison of the weight ratio of metal to consumed charge with and without CO sweep, as shown in Table 16, indicates that CO sweep decreases metal production during runs of limited duration due to increased reflux. Large amounts of slag which collected in the ingot in AF-14 corresponded to smaller accumulations of slag agglomerate in the reaction zone above the grate. Since a minor amount of ore drained into the metal reservoir during startup, AF-14 will be repeated in the near future. The CO ratios reported for the four CO sweep runs in Table 16 represent approximately 13% of the CO sweep that would be required in a three-atmosphere fully combustion heated reactor. This is based on the recent calculation for this hypothetical reactor wherein .267 gm of ore and reduction coke were charged for each gm of CO coming from burning carbon with O₂ to generate all the process heat. In terms of metal yield, AF-13 has the lowest CO sweep and yield indicating that either lower SiO₂/Al₂O₃ ratios give lower metal-plus-carbide yields of collectible product, or a different metal producing temperature is required to give better results. Temperature of metal production is another variable that must be studied in the future. In general, it appears that the SiO₂/Al₂O₃ ratio in the ore does not greatly affect metal yield and that metal can be easily produced with 13% of the CO sweep and 80% of the reduction carbon over a .5 to 1.0 ratio. Carbon stoichiometry and CO sweep are other variables that will be studied in the future.

Table 17 represents the various reduction carbon sources and the distribution of the carbon in the charge. In all cases, sufficient carbon was contained in the ore pellets to reduce all SiO₂ to SiC and only in AF-12 was no extra pet coke added to make the total carbon requirement. Within the conditions of these tests, it does not appear the source of carbon and location of carbon internal and external to

the ore pellet have drastic effects on the experimental results. It is also noted that the ore pellet sizes used were -3/8 +6 mesh and -6 mesh +10 mesh in AF-12 and AF-15 respectively, and that this variable does not seem to significantly affect the results.

Task completion is 30%.

Task No. 9: Supportive Analytical

A large number of samples were analyzed as required. A total of 422 man-hours were expended.

Task completion is 25%.

Task No. 10: Supportive Phase Identification

A series of metal alloy samples produced by carbothermic reduction on the 8-inch pilot VSR reactor were subjected to remelt experiments in order to determine the effectiveness of fractional melting for separation of Al-Si alloy from the carbides and Fe- and Ti- bearing intermetallics in the reactor product. The remelt samples were then submitted for phase analysis in order to determine the effects of fractional melting on the distribution of individual metallic phases.

SiC and $TiSi_2$ (Al, Fe) are concentrated in the refractory fractions, leaving a low-melting liquid slightly enriched in Al, Si, and Fe. Fe-Si-Al intermetallics are slightly enriched in the low-melting fraction; peritectic reactions with the melt resulted in the formation of $FeSiAl_5$ at the expense of high-temperature phases which have a lower Al content, reducing the amount of Al readily available for the formation of Al-Si alloy. In the low-iron metal samples, settling of intermetallic $FeSiAl_5$ crystals through the melt enriched the upper two thirds of the reservoir liquid in the Al-Si alloy. Crystal settling was not possible in the high-iron samples because of the small amount of low-melting liquid available (10-20% vs 55-70% in the low-iron samples).

Textural evidence indicates that the interfacial tension between the hypereutectic $FeSiAl_5$ crystals and the high-Al melt was sufficiently high to cause the hypereutectic $FeSiAl_5$

to crystallize as spherical grains, which then coalesced onto previously formed FeSiAl_5 crystals rather than remaining dispersed in the melt. Growth of large crystals of FeSiAl_5 by coalescence of smaller crystals should increase the efficiency of separation of FeSiAl_5 crystals from the Al-Si alloy by fractional crystallization, because the larger crystals will settle through the melt and accumulate at the bottom of the reservoir more rapidly than smaller grains. Hypereutectic Si, on the other hand, remains dispersed in the high-Al melt because of the low interfacial tension between Si and the melt.

Task completion is 25%.

Task No. 11: Supportive Mechanical Engineering

Machining activities were supplied as required. A total of 165 man-hours were expended.

Task completion is 30%.

B. ALLOY PURIFICATION - PHASE C

Task No. 1: Pilot Unit Installation

The design, fabrication, and purchasing of all major hardware items are complete i.e. the multipurpose furnace, furnace instrumentation/controls, crystallization vessel, crystallizer gas-fired heating systems, agitation system for the crystallizer, and the gas-fired holding ladle. All of the supporting equipment and tools have also been built, except for the false bottom product removal hardware which requires assembly.

Installation of the major hardware has been accomplished except for the agitation system. Most of the supporting systems' installations are also complete. Remaining to be installed are the electrical power supplied, the argon supply systems, the cooling air supply, product removal system, and miscellaneous instrumentation.

Task completion is 80%.

Task No. 2: Effects of Pilot Operating Parameters

Two areas were investigated during the past quarter: 1) impurity effects; and 2) reduction of iron levels by chemical means. The impurity effects experiments continued the study of copper additions to improve casting alloy yield, extending the iron content of the alloy above 10%. Past experimentation has shown that yields of up to 33% were possible with starting alloys of 30%Si-10%Fe-2%Cu-rem.Al. Current experimentation was not as successful, indicating that iron levels in excess of 10 wt% will create difficulties during the fractional crystallization process. Three experiments were performed, with initial compositions as follows:

Exp. 48	30%Si-10%Fe-2%Cu-rem. Al
Exp. 49	30%Si-15%Fe-2%Cu-rem. Al
Exp. 50	30%Si-15%Fe-4%Cu-rem. Al

Experiment 48 essentially was a repeat of Experiment 41, where a 30% yield was obtained. Experiment 48 had a 26% yield, a comparable result (see Table 18). Experiments 49 and 50 had increased iron contents, and the copper content was also varied. The yields were much lower, 8% and 2%, respectively (see Tables 19 and 20). The

lower yields suggest that copper additions can improve yields, but that there is a limit to their effectiveness at approximately 10% Fe. The results also indicate that a 2% Cu addition is an optimum level over a wide range of iron contents. See Table 21.

The copper additions reduce the iron level in the eutectic material and increase yield. To determine how this effect is achieved, phase analyses were performed on the crystal samples from Experiments 33 and 41, with initial compositions:

Exp. 33 30%Si-10%Fe-rem. Al
Exp. 41 30%Si-10%Fe-2%Cu-rem. Al

The phase analyses indicate that the copper does not form intermetallics with the iron or silicon, but is present as very small (<4 um) crystals in the aluminum matrix. It is possible that copper acts to lower the temperatures of the peritectic reactions between Al, Si, and Fe, leaving more liquid alloy at 590°C than is possible in the ternary Al-Si-Fe system.

The results of Experiments 49 and 50 indicate that some means of reducing iron levels to 10 wt% or lower is necessary if the reactor product iron levels cannot be reduced sufficiently by ore and carbon source selection. One method which has been briefly investigated is the use of a stripping solution to preferentially dissolve iron from an alloy. The success of this method would depend on several factors such as the surface area of alloy available to the stripping solution, the temperature of the solution, and the time in solution. Preliminary results were favorable. The tests were conducted at room temperature, with soaking times of 40 hrs and 72 hrs. In the experiment with the 72 hr soak, more aluminum was dissolved than was desired, indicating that a short soak time is preferable to a long soak. Further investigation of this technique would be warranted if reactor product iron contents will exceed 10-11% Fe.

This task is 25% complete.

Task No. 3: Pilot Unit Modifications

No progress.

Task completion is 0%.

Task No. 4: Supportive Analytical

Samples were analyzed as required. A total of 31 man-hours were expended.

Task completion is 25%.

Task No. 5: Supportive Mechanical Engineering

Work supporting Task No. 1 required 370 man-hours in this quarter.

Task completion is 30%.

C. PURIFICATION TO COMMERCIAL GRADE ALUMINUM
PHASE C

Task No. 1: Pilot Unit Installation

Quartz and graphite sleeves for the electrodes have been received and procurement of isolation chamber components is underway. A low permeability graphite is being sought for the isolation chamber. Inconel strips for the startup heaters were also received.

The components for the anode box (which holds the impure alloy) were cemented and screwed together and the system baked out. The membrane cloth was installed. The anode chamber was installed inside the cell, atop support structures consisting of graphite pillars and spacers. Spacers (which determine anode-cathode distance) were also positioned in the cell.

Other cell components that have been fabricated and installed include the graphite lid plate, top insulation, the steel lid and flanges, and the electrodes. Fabrication of the inconel strip heaters for startup is underway.

The product removal system is designed for vacuum tapping product aluminum from several regions of the cell. These regions provide access to the aluminum sump located beneath the anode chamber. The product removal equipment can also be used to remove concentrated alloy from the anode chamber or, in an emergency, the cell bath. For product removal, two alternatives are available. Molten aluminum can be cast into graphite crucibles centered within the vacuum chamber, or with considerably more preheating, tapped directly into the refractory-lined chamber for later pouring into molds. The jet ejector, transfer lines, and connections to the cell and vacuum chamber are similar to systems used commercially. The lid is sealed to a bottom section of the unit with flanges joined by swing bolts. The lid can therefore be quickly removed after tapping.

Procurement of this unit is underway. Steel fabrication for one lid and two bottom sections except for the flanges has been completed.

Several control functions are required for the membrane cell. The instrumentation requirements and logic for these systems has been determined. An important safety consideration is the prevention of sudden pressure surges to the cell which could force molten alloy out of the isolation chamber. It is important to maintain a positive nitrogen pressure within the cell, but excess pressure will cause the alloy to rise in the isolation chamber which is open to the atmosphere. Control functions and limits established to prevent pressure surges are as follows:

1. A photo-helic gauge/switch will monitor cell pressure and open a vent-valve if the cell pressure reaches 14 inches of water. Nominal operating pressure for the cell will be two to five inches of water.
2. Pressure regulators will be used in series in a main nitrogen line such that the failure of the last regulator will only allow a 5 PSIG surge. This nitrogen line will feed a manifold for all lid purges. A pressure switch will monitor pressure in the manifold and shut off a valve in the supply line if the pressure exceeds 20 inches of water.
3. Purges to the electrodes will be limited in pressure (2 PSIG) and flow as required to prevent excess pressures in the cell. A manifold pressure switch will also be used in this system.

Control functions are also required for pressure tapping bath into the cell, vacuum tapping of product aluminum, and temperature control for all heated units. Control of the tapping operations will be based on bath depth measurements within the cell.

Procurement of instrumentation and measuring devices is nearly complete. Design of electrical circuitry and construction of panels has been initiated.

The bath melter will be used to melt bath, filter out insolubles, and transfer molten bath to the cell. It consists of an inner inconel container (designed for pressure tapping) surrounded by a resistance heating system, insulation and an outer steel shell. During this period, the insulation and resistance heating coils were installed in the unit. The inconel crucible and lid were fabricated and also installed.

One inconel filter system has been built.

Task completion is 35%.

Task No. 2: Effects of Pilot Operating Parameters

No progress.

Task completion is 0%.

Task No. 3: Pilot Unit Modifications

No progress.

Task completion is 0%.

Task No. 4: Support Pilot Operations

The nominal bath composition for start-up of the cell has been changed for 90% LiCl, 10% AlCl₃, to 45% LiCl, 45% NaCl, 10% AlCl₃, in order to reduce the risks associated with the very high LiCl bath. These include higher volatility, greater penetration of the refractory wall, and higher and more uncertain heat transfer losses. The new bath will require an increase in operating temperature of the bath melter from 620°C-660°C to 660°C-700°C, because of a higher liquidus point.

Graphite cements were tested to determine if the bond for the membrane cloth would be adequate. Once bench scale techniques were applied, reasonably strong bonds were obtained with C-38 cement.

Two other cements (C-34 and #551 adhesive) tended to powder, and very little bond strength was obtained.

Electrode polarization contributed very significantly to the cell voltage in previous bench-scale experimentation. A bench-scale cell was constructed to study the polarization effects with the aim to reduce their impact in pilot cell operation.

The limit at which metal starts penetrating the membrane

was established for one set of conditions in an experiment set up as shown in Figure 7.

A piece of the membrane is attached to the end of a graphite tube. Metal is placed into the tube, which is immersed in electrolyte. An inert gas pressure is applied until the metal is observed to penetrate the membrane.

For a G5502 continuous filament (FMI) graphite cloth, a penetration pressure of 2.3 psi was established with aluminum in a 90% LiCl-10% AlCl₃ electrolyte at 725°C. The end of the tube was immersed about one-in. into the bath.

The observed pressure of 2.3 psi would correspond to the pressure produced by 180 cm of aluminum, i.e., it corresponds to the pressure at the bottom of a 180 cm deep aluminum layer which is counterbalanced by a 180 cm deep layer of electrolyte.

Task completion is 50%.

Task No. 5: Supportive Analysis

Samples were analyzed as required.

Task completion is 25%.

Task No. 6: Supportive Mechanical Engineering

Mechanical engineering assistance was provided for Task No. 1. A total of 59 man-hours were expended.

Task completion is 50%.

PHASE C SECOND QUARTER PROGRAM

Administrative

Increased expenditure limits for subcontractors will be requested to cover Phase C work. Alcoa will request additional DOE funding to support a projected cost overrun.

Technical

Reduction: Magnetic separation techniques will be evaluated for reducing Fe and Ti concentrations in bauxite. The VSR pilot reactor will be modified and operated to facilitate evaluation of a blast-arc concept as an alternative to reduction in a blast furnace. Continuous tapping of metal alloy produced in the pilot unit will be attempted. Flow sheets for a commercial blast-arc process will be developed. Further development of the SOLGASMIX computer program is planned, with a visit scheduled by Messrs. Erikkson and Johansson of Sweden, to exchange technology in this field. The bench-scale reactor will be operated to study the effects of CO sweep and $\text{SiO}_2/\text{Al}_2\text{O}_3$ ratio on metal yield. Carbon solubility in Al-Si alloys will also be determined. Pilot and bench reactor products will be analyzed in detail by microscopic techniques.

Alloy Purification: The pilot crystallizer assembly and installation will be completed. The unit will be started up.

Purification to Commercial Grade Aluminum: Various pilot cell construction and installation items will be worked on, including the product removal system, shell piping, bath melter, and electrical buswork system.

Cost Summary

Expenditures for the first three months of Phase C totalled \$483,200. Distribution was \$282,667 for Reduction,

\$90,762 for Alloy Purification, and \$109,774 for Purification to Commercial Grade Aluminum. Total cumulative spending through the first 31 months of the contract was \$3,879,214. Actual spending for Phase C is compared to estimated spending in Attachment 1.

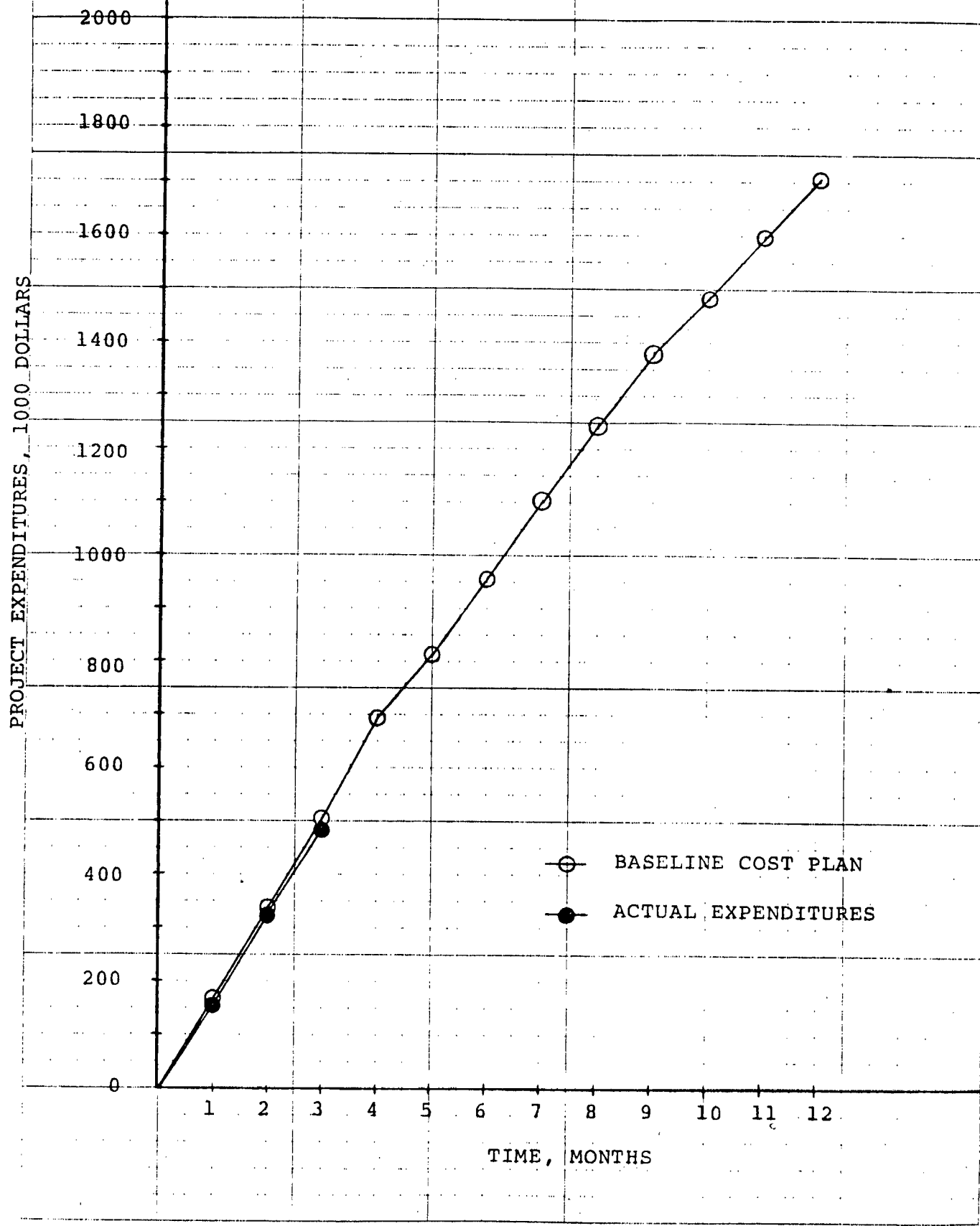
Assigned Personnel

The actual man-hrs expended by engineers and technicians for the first quarter of Phase C are shown in Attachment 2 and compared to estimated man-hrs. For engineers, actual was 19.3% above estimated. For technicians, actual was 1.1% below estimated. Total cumulative man-hrs were 4.8% above estimated.

Task/Milestone Schedule

Attachment 3 shows the task-time relationship for the three major tasks from initiation in DOE fiscal year 1977 (fourth quarter) through completion of the current contract in DOE fiscal year 1981 (first quarter). Completed milestones are noted by filled-in circles.

ATTACHMENT 1
PHASE C COST CHART



ATTACHMENT 2

PHASE C MAN-HOUR SUMMARY

	<u>FIRST QUARTER</u>	<u>SECOND QUARTER</u>	<u>THIRD QUARTER</u>	<u>FOURTH QUARTER</u>	<u>CUMULATIVE</u>	<u>CUMULATIVE</u>		
	<u>ACTUAL</u>	<u>EST.</u>	<u>ACTUAL</u>	<u>EST.</u>	<u>ACTUAL</u>	<u>EST.</u>	<u>% DEVIATION</u>	
ENGINEERS	3227	2705				3227	2705	+19.3
TECHNICIANS	<u>6464</u>	<u>6539</u>	—	—	—	<u>6464</u>	<u>6539</u>	<u>- 1.1</u>
TOTAL	9691	9244				9691	9244	+ 4.8

ALUMINUM COMPANY OF AMERICA

ALCOA LABORATORIES

Attachment 3

Direct Reduction Project

Legend for symbols:

- Milestone reached
- Milestone planned
- ▲ Milestone proposed

Project Milestones:

- Contract Procurement:**
 - FY 77: Contract Awarded (▲)
 - FY 78: Computer Prog. Heat, Mass Bal. (●)
 - FY 79: Detailed High Temp. Furnace (●)
 - FY 80: Installed High Temp. Furnace (●)
 - FY 81: Scale-up (●)
 - FY 82: Complete Demo. Plant Design (△)
 - FY 83: Demo. Plant Installation, Start-up (△)
 - FY 84: Start-up (△)
 - FY 85: Plant Install. (△)
 - FY 86: Plant Install. (△)
 - FY 87: Plant Install. (△)
 - FY 88: Plant Install. (△)
 - FY 89: Plant Install. (△)
 - FY 90: Complete commercial plant start-up (△)
- Reduction:**
 - FY 77: Reduction of Impurities in Production Pilot Unit (●)
 - FY 78: Designed Pilot Unit (●)
 - FY 79: Installed Pilot Unit (●)
 - FY 80: VSR-1 Start-up (●)
 - FY 81: VSR-2 Start-up (●)
 - FY 82: VSR-3 Start-up (●)
- Alloy Purification:**
 - FY 77: Pilot System Start-up (●)
 - FY 78: Design Pilot Unit (●)
 - FY 79: Install. Pilot Start-up (○)
 - FY 80: Scale-up Design (○)
- Purification to Commercial Purity Al:**
 - FY 77: Pilot Efficiency (●)
 - FY 78: Pilot Efficiency (●)
 - FY 79: Pilot Efficiency (●)
 - FY 80: Pilot Efficiency (○)
 - FY 81: Scale-up Design (○)
 - FY 82: Scale-up Design (○)
 - FY 83: Scale-up Design (○)
 - FY 84: Scale-up Design (○)
 - FY 85: Scale-up Design (○)
 - FY 86: Scale-up Design (○)
 - FY 87: Scale-up Design (○)
 - FY 88: Scale-up Design (○)
 - FY 89: Scale-up Design (○)
 - FY 90: Scale-up Design (○)

TABLE 1
BURDEN MATERIAL PREPARED IN 1980 FOR DIRECT REDUCTION
(74D1450601)

<u>EXPT. NO.</u>	<u>BOOK AND PAGE NO. METHOD</u>	<u>RAW MATERIALS USED</u>			<u>CARBON</u>	<u>QUANTITY</u>	<u>SIZE</u>	<u>YIELD</u>	<u>FIRRED COMPRESSIVE STRENGTH</u>
5A1091	EIRICH BALLS 19185-18	64.331 H. CLAY (64.331%)	10.375 B. BXTE. (10.375%)	25.294 COED. CHAR. (25.294%)	1.0 OXIDE RATIO @80% RED. CARB.	100#	3/8" x 6M		298.0#/sq in
5A1092	EIRICH BALLS 19185-19	H. CLAY (39.033%)	B. BXTE. (37.445%)	COED. CHAR. (23.522%)	.5 OXIDE RATIO @80% RED. CARB.	100#	3/8" x 6M		217#/sq in
5A1097	EIRICH BALLS 19185-20	276.51 H. CLAY (55.302%)	100.185 B. BXTE. (20.037%)	123.305 COED. CHAR. (24.661%)		500#	3/8" x 6M	63.9%	139.5# sq in 1/4" dia
5A1103	SMALL DISK 19185-31	9.52 H. CLAY (75.19%)	3.14 COED. CHAR. (24.80%)			12.66#	3/8" x 6M		98.72#/sq in
5A1105	SMALL DISK 19185-32	6.97 H. CLAY (55%)	2.55 B. BXTE. (20.14%)	3.14 COED. CHAR. (24.8%)		12.66#	3/8" x 6M		

TABLE 2

AUGER PERFORMANCE

Run	Auger Length	Auger Bottom to Tuyere	Grate Position Relative to Tuyere	RPM	Miscellaneous	Reason for Failure
VSR-3-28	1 piece auger w/ slots	20"	-2-1/2"	2.0/2.2	Rebuilt reactor with new .4" I.B.tuyeres, -3/8" + .203 met coke and 40 SCFH O ₂ /tuyere in use. Same ore mixture and shear pin arrangement as in VSR-3-27	Shutdown due to shear pin failure after 50 slugs of ore were fed.
VSR-3-29	1 piece auger 17" with slots		-2-1/2"	2.1	Same conditions as VSR-3-28 but with auger 3" lower and 5A1075 ore now in use. New auto transformer.	Shutdown due to shear pin failure after 11 slugs of ore were fed.
VSR-3-30	1 piece auger 17" with slots		-2-1/2"	2.0/2.07	Same conditions for the auger as in VSR-3-29, but with -3/8" + .203 met coke and 30 CFH O ₂ /tuyere in use. The ore mixture of 73% 5A1063/27% 5A1068 was used. Auger shear pins were considerably strengthened to leave only a small margin of stress between failure of the shear pin and the auger.	No auger failure, but the bed movement was cut off by a severe bridge below the bottom of the auger. Auger disassembly broke in
VSR-3-31	New auger, same shape as original 1 piece auger used in VSR-3-23 and without slots. Joint in blank at top of flutes.	15"	-2-1/2"	2.0	Rebuilt reactor with old tuyere .375" I.D. and -1/4" joint in top of + 6 mesh met coke. Cut O ₂ rate to 25 CFH/tuyere. Same ore mixture used as in VSR-3-30	Auger failed at joint in top of auger, possibly while attempting to break crust on top of bed. A severe bridge formed around the auger above the bottom and partially filling up the flutes and cutting off the flow of the bed.

TABLE 3

OVERALL MASS BALANCE SUMMARY FOR PILOT REACTOR COMBUSTION RUNS

VSR	O ₂ RATE CFH @ 20°C	O ₂ TIME HRS	TOTAL COKE G	TOTAL ORE G	TOTAL O ₂ G	INITIAL CHARGE G	FINAL BED WEIGHT G	CONSUMED CHARGE O ₂	O ₂ RATIO
23	240	5.417	45182	15818	48978	21356	19701	.843	1.443
24	240	7.417	58509	28840	67061	21500	27632	.890	1.367
26	120	3.183	16343	12523	14390	20616	22990	.408	2.980
27	120	5.950	36023	15180	26899	17393	23609	1.026	1.186
28	120	5.350	29568	17111	24186	18327	25942	.857	1.419
29	120	4.383	31538	5399	19815	17974	19025	.904	1.346
30	90	3.583	27057	11630	12148	16766	17480	1.746	.697
31	75	5.633	24596	19647	15916	16278	19873	1.531	.795

O₂ Ratio = $\frac{\text{O}_2 \text{ supplied in pilot reactor test}}{\text{O}_2 \text{ required to fully combustion heat a 3 atm. shaft furnace}}$

Consumed Charge = Total Coke + Total Ore - Final Bed Weight.

TABLE 4
ELECTRIC HEATED PROCESS, $P = \text{ONE ATMOSPHERE}$
BASIS = 1 MOLE Al_3Si_2

	Al_2O_3		C	SiO_2	SiC	$\text{Al}_4\text{O}_4\text{C}$	Al_3Si_2	CO	SiO	Al	Al_2O	
	1.50		8.60	2.07								
I.												
$T = 1840^\circ\text{K}$	1.58		2.54		2.08			8.59	.05			
II.												
$T = 2205^\circ\text{K}$					2.22	.87		4.61	.07	.04	.06	
III.												
$T = 2300^\circ\text{K}$							1.00	3.07	.21	.10	.18	

TABLE 5

HEAT BALANCE BY STAGES - 100% ELECTRIC, ONE ATMOSPHERE
BASIS = 1 MOLE Al_3Si_2 (81g Al)

PREHEAT

<u>REACTANTS</u>	<u>TEMP. RANGE, °K</u>	<u>MOLES</u>	<u>KG</u>	<u>KJ/MOLE</u>	<u>ΔH</u>	<u>HEAT KJ</u>
Al_2O_3	300 - 1840	1.50		187.52		+281.28
SiO_2	300 - 1840	2.07		107.99		+223.53
C	300 - 1840	8.60		31.33		+269.46
CO*	1840 - 300	8.59		50.45		<u>-433.39</u>
						+340.88

STAGE I

$ΔH^R$	1840	0.5178	2136.59	+1106.33
--------	------	--------	---------	----------

STAGE II

$ΔH^R$	2205	0.3857	1588.93	+612.85
Al_2O_3	1840 - 2205	1.58	50.41	+ 79.59
SiC	1840 - 2205	2.08	19.71	+ 41.01
C	1840 - 2205	2.54	9.00	+ 22.92
CO*	2205 - 1840	4.61	13.26	<u>- 61.14</u>
				+695.23

STAGE III

$ΔH^R$	2300	0.2483	7019.78	+1743.01
Al_4O_4C	2205 - 2300	.866	25.84	+ 22.38
SiC	2205 - 2300	2.22	5.19	+ 11.53
CO	2300 - 2205	3.07	3.48	<u>- 10.70</u>
				+1766.22

Net Heat (Electric) = 3908.66

-38-
TABLE 6

HEAT BALANCE BY STAGES - HYBRID, ONE ATMOSPHERE
BASIS = 1 MOLE Al_3Si_2 (81g Al)

<u>PREHEAT</u>		<u>ΔH</u>			
<u>REACTANTS</u>	<u>TEMP. RANGE °K</u>	<u>MOLES</u>	<u>KG</u>	<u>KJ/MOLE</u>	<u>KJ/KG</u>
Al_2O_3	300 - 1840	1.50		187.52	+281.28
SiO_2	300 - 1840	2.19		107.99	+236.50
C	300 - 1840	8.70		31.33	-272.57
CO	1840 - T_{exit}	28.39		27.84	<u>-790.35</u>
					0
<u>COMBUSTION</u>					
ΔH_R	1840	19.9		59.61	-1185.96
<u>STAGE I</u>					
ΔH_R	1840		1.0805	1097.6	+1185.96
<u>STAGE II</u>					
ΔH_R	2205		.03857	1588.93	+612.85
Al_2O_3	1840 - 2205	1.58		50.41	+ 79.59
SiC	1840 - 2205	2.08		19.71	+ 41.01
C	1840 - 2205	2.54		9.00	+ 22.92
CO	2205 - 1840	4.61		13.26	<u>- 61.14</u>
					+695.23
<u>STAGE III</u>					
ΔH_R	2300		0.2483	7019.78	+1743.01
$\text{Al}_4\text{O}_4\text{C}$	2205 - 2300	.866		25.84	+ 22.38
SiC	2205 - 2300	2.22		5.19	+ 11.53
CO	2300 - 2205	3.07		3.48	<u>- 10.70</u>
					+1766.22
Net Heat (Electric) = 2461.45					

TABLE 7

COMBUSTION HEATED PROCESS, $P = \text{three atmospheres}$, $T_b = 630^\circ\text{K}$
BASIS = 1 MOLE Al_3Si 1.29

TABLE 8

ORE, ALLOY AND BY-PRODUCT MATERIALS BALANCE
BASIS = 100g ORE

<u>ORE</u>	<u>ALLOY</u>			<u>BY-PRODUCTS, g/100g ore</u>				<u>NET</u>		
<u>Constituent</u>	<u>%</u>	<u>Constituent</u>	<u>%</u>	<u>g</u>	<u>100g ORE</u>	<u>TiSi₂</u>	<u>SiC</u>	<u>FeSiAl₅</u>	<u>Si</u>	<u>Al</u>
SiO ₂	29.77	Si	35.9	13.89		1.21	5.32	0.70	6.66	
Fe ₂ O ₃	1.99	Fe	3.6	1.39				1.39		
TiO ₂	1.74	Ti	2.7	1.04		1.04				
Al ₂ O ₃	37.96	Al	51.9	20.01				3.35		16
C	<u>28.54</u>	C	<u>5.9</u>	<u>2.28</u>			<u>2.28</u>			
	100.0		100.0	38.70		2.25	7.60	5.44	6.66	16

$$\text{SiO}_2/\text{Al}_2\text{O}_3 = 0.79 \quad \text{Al/Si} = 1.45 \quad (\sim 60/40) \quad \text{g, ore/g.Al} = \frac{1}{.1675} = 5.97$$

Alloy Yield = 38.7% Aluminum Yield = 16.75%

TABLE 9
ENERGY CREDITS FOR BY-PRODUCTS

ELECTRIC ENERGY

	<u>g/100g</u> <u>ore</u>	<u>moles</u> <u>100g ore</u>	<u>SiC</u>	<u>SiO₂</u>	<u>CO₂</u>	<u>Fe₂O₃</u>	<u>Al₂O₃</u>	<u>TiO₂</u>	<u>TOTAL</u>
SiC	7.60	0.1900	[+66.94	-910.44	-393.51] -235.03
FeSiAl ₅	5.44	0.0248	[-910.44	-410.66	-4193.41] -136.76
TiSi ₂	2.25	0.0216	[-1820.88			-944.75	-	59.74
Si	<u>6.66</u>	0.2379	[-910.44] <u>-216.59</u>
	21.95								-648.12
	(6.4812) (5.97) ÷ .425 =								91.04
	<u>KJ</u> <u>g ore</u>	<u>g ore</u> <u>g Al</u>							<u>KJ/g_A</u>

COAL ENERGY

$$(5.97) [(0.1900) (2) + (0.0248) (12) + (0.0216) (6) + (0.2379) (2)]$$
$$\frac{12}{(100) (.8)} (32.79) = 37.67$$
$$\frac{g \text{ ore}}{g \text{ Al}} \left[\frac{\text{moles}}{100 \text{ g}} \times \frac{\text{mole C}}{\text{mole ore}} + \dots \right] \frac{100 \text{ g}}{\text{g}} \cdot \frac{\text{g C}}{\text{mole}} \cdot \frac{\text{KJ}}{\text{gC}} = 128.71$$

TOTAL ENERGY = 129 KJ/g Al

TABLE 10

ENERGY REQUIREMENTS FOR ELECTRIC, HYBRID, AND COMBUSTION PROCESSES

ELECTRIC PROCESS

Electric Energy:

$$[\frac{3908.66}{(81)(.90)} + 2.3 + 10.1 + 2.78 + 18.6] / .425 = \frac{KJ/gAl}{181.9}$$

(See Table 2) Fe, Ti, pellets refining C purification efficiency

Coal Energy:

$$(5.98)(.2854)(32.79) / .8 = \frac{70.0}{\text{Reduction \& Solution}}$$

CO Credit:

$$(5.98)(.2626)(23.59) = \frac{-37.0}{\text{Reduction}}$$

Metalloid
By-Product
Credit

-129.0

= 109.7

HYBRID PROCESS

Electric Energy:

$$[\frac{2461.45}{(81)(.90)} + 2.3 + 10.1 + 2.78 + 18.6 + \frac{(19.9)(16)(1.32)}{81}] / .425 = \frac{171.1}{}$$

(See Table Fe, Ti, pellets refining C purification O_2 plant
3) O_2 plant

Coal Energy:

$$[(19.9)(12)/81 + (5.98)(.2854)](32.79) / .8 = \frac{190.8}{\text{combustion reduction \& solution}} \frac{361.9}{}$$

CO Credit:

$$[(19.9)(12)/81 + (5.98)(.2626)](23.59) = \frac{-106.6}{\text{combustion reduction}}$$

Metalloid
By-Product
Credit

= -129.0

126.3

TABLE 10
Continued

COMBUSTION PROCESS

Electric Energy:

$$[2.3 + 10.1 + 2.78 + 18.6 + \frac{(84.64)(16)(1.32)}{81}] + .425 = 131.4$$

Coal Energy:

$$[(84.64)(12)/81 + (5.98)(.2854)](32.79/.8) = \frac{583.9}{715.3}$$

CO Credit:

$$[(84.64)(12)/81 + (5.98)(.2626)] (23.59) = -332.8$$

Metalloid
By-Product
Credit

$$= \frac{-129.0}{253.5}$$

TABLE 11
 COMPARISON OF ENERGY REQUIREMENTS FOR VARIOUS
 PROCESSES FOR PRODUCING ALUMINUM

		Energy Requirements, KJ/g. (kWhr/#)					
<u>Process</u>	<u>Fuel</u>	<u>Electric Equiv.</u>	<u>Coal</u>	<u>Total</u>	<u>CO Credit</u>	<u>Credit for Ferrosilicon</u>	<u>Net</u>
Electric	Coke	205.7 (11.0)	70.0	275.7	37.0	129.0	109.7
	Coal	205.7 (11.0)	56.0	261.7	37.0	129.0	95.7
	Coal, CO* Credit for Electricity	175.2 (9.4)	56.0	231.2	0	129.0	102.2
Hybrid	Coke	171.1 (9.2)	190.8	361.9	106.6	129.0	126.3
	Coal	171.1 (9.2)	152.6	323.7	106.6	129.0	88.1
	Coal, CO* Credit for Electricity	83.3 (4.5)	152.6	235.9	0	129.0	106.9
Combustion	Coke	131.4 (7.0)	583.9	715.3	332.8	129.0	253.5

*CO credit for generating electricity at 35% efficiency.

TABLE 12

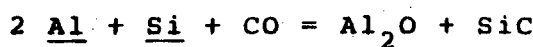
STAGE III EQUILIBRIUM EQUATIONS



$$K_1 = e^{(-484918 + 194.203 T)/RT}$$

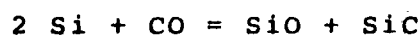
$$\underline{\text{Al}} = \underline{\text{Al}}_{(g)}$$

$$K_2 = e^{(-72018 + 24.748T)/RT}$$



$$K_3 = e^{1975 (45333 - 18.794T)/RT}$$

$$K_3 = e^{1972 (48800 - 21.846T)/RT}$$



$$K_4 = e^{(40117 - 17.728T)/RT}$$

$$P_{\text{CO}} = [K_1 / (\underline{\text{Al}}^4 \underline{\text{Si}}^3)]^{1/4}$$

$$P_{\text{Al}} = K_2 \underline{\text{Al}}^a$$

$$P_{\underline{\text{Al}}_2\text{O}} = K_3 P_{\text{CO}}^a \underline{\text{Si}}^a \underline{\text{Al}}^2$$

$$P_{\text{SiO}} = K_4 \underline{\text{Si}}^a P_{\text{CO}}^2$$

$$\bar{Z} P_i = P_T$$

TABLE 12
Continued.

MASS BALANCES: ONE-PASS YIELDS FOR STAGE III

Basis = 1 mole of gas ($P_i = N_i$)

$$\begin{aligned}
 N_t^{Al} &= P_{CO} + P_{Al_2O} + P_{SiO} & N_t^{Si} &= \frac{3}{4} (P_{CO} + P_{Al_2O} + P_{SiO}) \\
 N_g^{Al} &= P_{Al} + 2P_{Al_2O} & N_g^{Si} &= P_{SiO} \\
 N_1^{Al} &= N_t^{Al} - N_g^{Al} & N_s^{Si} &= P_{Al_2O} + P_{SiO} \\
 &= P_{CO} - P_{Al_2O} + P_{SiO} - P_{Al} & N_1^{Si} &= N_s^{Si} - N_g^{Si} - N_s^{Si} \\
 Y_{Al} &= \frac{N_1^{Al}}{N_t} = \frac{P_{CO} - P_{Al_2O} + P_{SiO} - P_{Al}}{P_{CO} + P_{Al_2O} + P_{SiO}} & &= \frac{3/4 P_{CO} - 1/4 P_{Al_2O} - 5/4 P_{SiO}}{N_t^{Si} - N_s^{Si}} \\
 & & Y_{Si} &= \frac{N_1^{Si}}{N_t^{Si} - N_s^{Si}} \\
 & & &= \frac{3P_{CO} - P_{Al_2O} - 5P_{SiO}}{3P_{CO} - P_{Al_2O} - P_{SiO}}
 \end{aligned}$$

TABLE 13

COMPARISON OF CALCULATED PARTIAL PRESSURES AND ONE-PASS
YIELDS FOR VARIOUS VALUES OF $\Delta G_f^{Al_2O}$, A_{Al} , and A_{Si}

Al_2O Data	1972	1975	1975	1975	SOLGASMIX
A_{Al}	0.6	0.6	.54	.38	SOLGASMIX
A_{Si}	0.4	0.4	.36	.32	SOLGASMIX
P_{CO}	.7938	.7269	.7737	.8463	.8628
P_{Al}	.0572	.0543	.0455	.0260	.0273
P_{Al_2O}	.0638	.1338	.1087	.0597	.0512
P_{SiO}	.0883	.0833	.0747	.0725	.0580
Y_{Al} , %	80.5	65.9	72.5	85.2	86.6
Y_{Si} , %	84.2	83.0	86.0	87.9	90.5
T_1 °K	2359	2351	2340	2309	2300

TABLE 14
METALLOGRAPHIC PHASE ANALYSIS IN VOLUME %

RUN	% TOTAL CARBON	ORE $\text{SiO}_2/\text{Al}_2\text{O}_3$	WT. BASIS	UNCOALESCED METAL			
				SLAG	Si	SiC	Al_4SiC_4
AF-7	100%		.6	--	16	12	2
AF-12	80		.784	9	15	15	--
AF-13	80		.502	6	19	17	1
AF-14	80		.993	2	18	22	--
AF-15	80		.788	3	16	11	--

RUN	METAL BELOW SLAG LAYER				METAL ABOVE SLAG LAYER				TOP METAL			
	SLAG	Si	SiC	Al_4SiC_4	SLAG	Si	SiC	Al_4SiC_4	SLAG	Si	SiC	Al_4SiC_4
AF-7	2	18	31	9	2	14	30	2	--	27	10	2
AF-12	10	21	18	--	--	15	31	--	--	20	15	--
AF-13	5	15	23	3	1	18	16	6	1	20	11	2
AF-14	20	9	53	--	--	24	9	--	--	25	2	--
AF-15	16	16	23	--					--	24	11	--

These data are taken from the following letter reports by Steve Libby - Extractive Metallurgy Division
 Phase Analysis AF-7, S.C. Libby to D.T. Stevenson, 1980-05-21
 Phase Analysis AF-12, S.C. Libby to D.T. Stevenson, 1980-04-10
 Phase Analysis AF-13, S.C. Libby to D.T. Stevenson, 1980-04-14
 Phase Analysis AF-14, S.C. Libby to D.T. Stevenson, 1980-04-17
 Phase Analysis AF-15, S.C. Libby to D.T. Stevenson, 1980-05-05

TABLE 15

ORE SI/AL COMPARED TO METAL COMPOSITION

<u>RUN</u>	<u>ORE Si/Al WT. BASIS</u>	<u>FIRST METAL Si/Al</u>	<u>C</u>	<u>LAST METAL Si/Al</u>	<u>C</u>
AF7	.53	.43	5.93	.45	4.91
AF8	.56	.48	8.17		
AF10	.692	.54	8.44		
AF11	.692	.39	4.79		
AF12	.692	.59	7.67	.60	6.91
AF13	.443	.38	6.67	.51	8.88
AF14	.877			.66	4.40
AF15	.696	.44	2.75	.58	8.63

TABLE 16

EFFECT OF $\text{SiO}_2/\text{Al}_2\text{O}_3$ AND CO SWEEP ON METAL PRODUCTION

RUN	ORE $\text{SiO}_2/\text{Al}_2\text{O}_3$ WT. BASIS	CONSUMED CHARGE CO	CO RATIO	WT. METAL CONSUMED CHARGE	REACTION ZONE WT.	METAL PRODUCING TEMPERATURE
AF7	.6	--	--	.210	--	2050
AF12	.784	1.815	.147	.164	1280 gm	2050
AF13	.502	2.199	.121	.161	1341	2055
AF14	.993	2.035	.131	.177	759	2060
AF15*	.788	1.950	.137	.191	718	2065

CO RATIO =
$$\frac{\text{CO SUPPLIED IN BENCH SCALE REACTOR TEST}}{\text{CO FROM FULL COMBUSTION HEATING A 3 ATM SHAFT FURNACE}}$$

CONSUMED CHARGE = TOTAL ORE FED - REMAINING LOOSE CHARGE IN THE AUGER.

*because the bed was run so low at the end of AF15 as compared to AF12, the consumed charge of AF15 was increased by the difference in the weights of the partially reacted burden found below the auger in AF12 and AF15. This amounted to a 562 gm increase in the results of AF15 for a total weight of 10388 gm for the estimated consumed charge.

TABLE 17
CARBON STOICHIOMETRY OF ORE BURDEN

<u>RUN</u>	<u>BASIS</u>	<u>ORE</u>	<u>% C FOR SiC</u>	<u>% TOTAL C</u>	<u>CARBON SOURCE</u>
		<u>SiO₂/Al₂O₃</u> <u>WT.</u>			
AF7	.6	71.0%	58%	~100%	met and pet coke
AF12	.784	80.55%	67%	80.55%	met coke
AF13	.502	64.24%	51%	80.0%	char and pet coke
AF14	.993	63.75%	76%	80.0%	char and pet coke
AF15	.788	56.74%	67%	80.0%	char and pet coke

TABLE 18
BENCH SCALE RESULTS
EXPERIMENT 48

	<u>Weight, g</u>	<u>Content, %</u>		
		<u>Si</u>	<u>Fe</u>	<u>Cu</u>
Starting alloy after sampling and skim removal	2619.4	28.4	10.7	1.9
Drain (590°C)	120.4	16.4	3.2	3.5
Remelt Cut #1 (700°C)	272.0	17.1	2.5	3.3
#2 (760°C)	296.0	23.1	5.3	2.6
#3 (840°C)	818.0	23.7	5.6	2.8
#4 (940°C)	699.0	28.9	14.6	0.9

	<u>Content, %</u>	<u>Cumulative Yield, %</u>	<u>Avail. Al Recovered, %</u>
	<u>Si</u> <u>Fe</u> <u>Cu</u>		
Drain	16.4 3.2 3.5	4	6
Drain + 1	16.9 2.7 3.4	15	20
Drain + 1, 2	20.0 3.8 3.0	26	33

TABLE 19

BENCH SCALE RESULTS

EXPERIMENT 49

	<u>Weight, g</u>	<u>Content, %</u>	<u>Si</u>	<u>Fe</u>	<u>Cu</u>
Starting alloy after sampling and skim removal	2590.7		26.8	13.9	1.9
Drain (590°C)	22.6		17.8	4.6	4.5
Remelt Wt #1 (700°C)	93.0		20.2	6.8	4.3
#2 (760°C)	92.0		21.8	4.4	3.8
#3 (840°C)	590.8		25.5	8.2	3.1
#4 (940°C)	1595.9		31.2	19.8	1.0

	<u>Content, %</u>	<u>Cumulative Yield, %</u>	<u>Avail. Al Recovered, %</u>
	<u>Si</u>	<u>Fe</u>	<u>Cu</u>
Drain	17.8	4.6	4.5
Drain + 1	19.7	6.4	4.3
Drain + 1, 2	20.6	5.5	4.1

TABLE 20
BENCH SCALE RESULTS
EXPERIMENT 50

	<u>Weight, g</u>	<u>Si</u>	<u>Fe</u>	<u>Cu</u>
Starting alloy after sampling and skim removal	2545.2	27.8	13.7	4.0
Drain (590°C)	--	--	--	--
Remelt Cut #1 (700°C)	65.7	18.9	3.3	7.5
#2 (760°C)	279.2	24.7	7.5	6.5
#3 (840°C)	1201.4	26.1	9.6	16.0
#4 (940°C)	722.0	27.1	16.0	2.4

	<u>Content, %</u>	<u>Cumulative Yield, %</u>	<u>Avail Al Recovered, %</u>
	<u>Si</u> <u>Fe</u> <u>Cu</u>		
Drain	18.9 3.3 7.5	2%	3%

TABLE 21

COMPARISON OF YIELD

SUMMARY OF FE-HANDLING TECHNIQUES EXPERIMENTS

FE CONTENT 10% OR GREATER

<u>Experiment</u>	<u>Starting Alloy Content, %</u>				<u>Comments</u>
	<u>Si</u>	<u>Fe</u>	<u>Cu</u>	<u>Mg</u>	
26	29.2	10.2	--	--	
34	31.6	15.3	--	--	Pooled high Fe cuts
35	28.5	14.5	--	--	Stop at 820°C
40	31.2	10.3	4.4	--	Cu addition
41	31.0	9.4	1.9	--	Cu addition
48	28.4	10.7	1.9	--	Cu addition
49	26.8	13.9	1.9	--	Cu addition
50	27.8	13.7	4.0	--	Cu addition

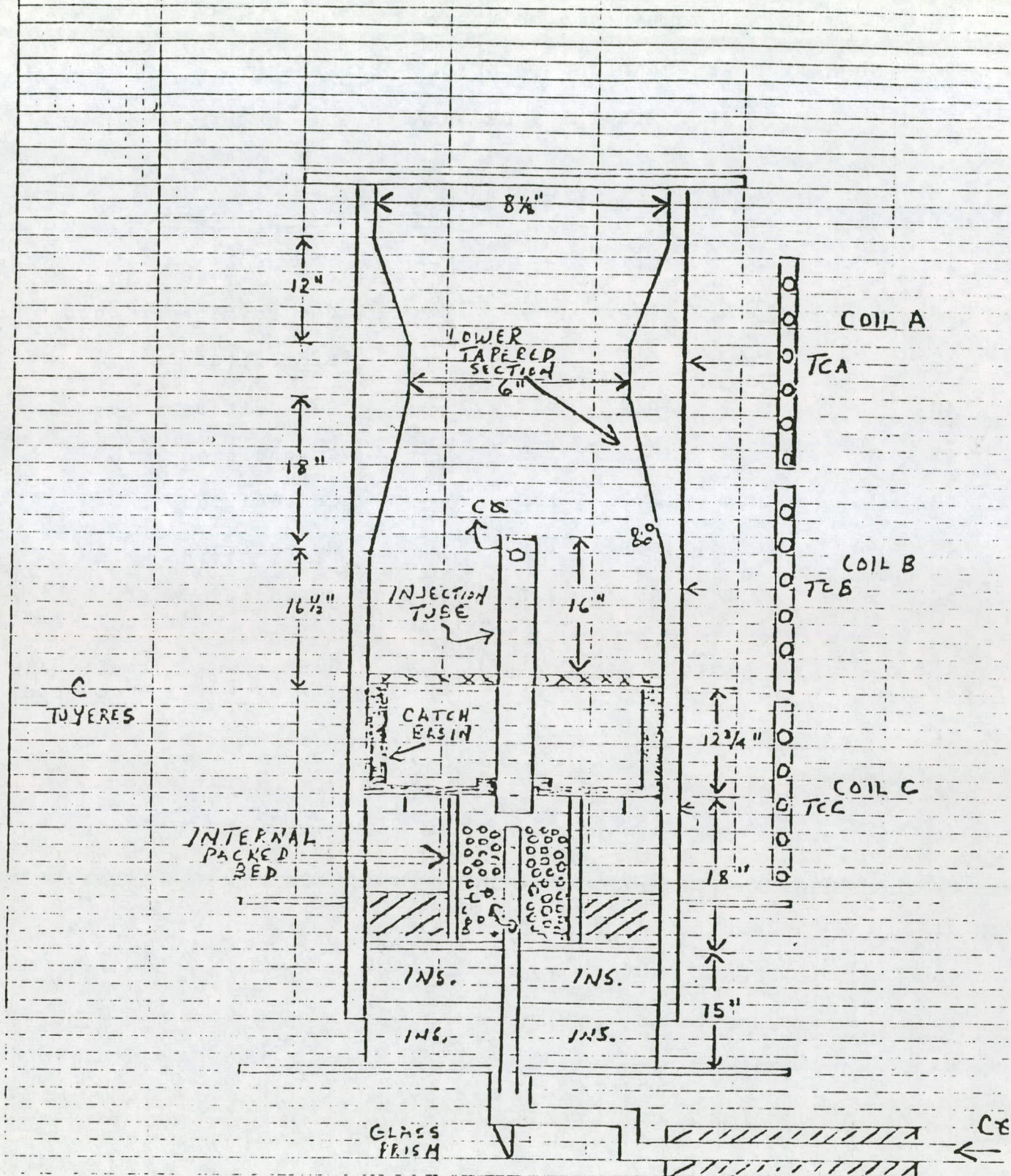
<u>Experiment</u>	<u>Casting Alloy Content, %</u>				<u>Cumulative Yield, %</u>	<u>Avail. Al Recovered, %</u>
	<u>Si</u>	<u>Fe</u>	<u>Cu</u>	<u>Mg</u>		
26	14.1	1.1	--	--	<1	1
34	--	--	--	--	--	--
35	--	--	--	--	--	--
40	19.3	3.7	6.3	--	28	37
41	20.0	3.8	3.0	--	31	39
48	20.0	3.8	3.0	--	26	33
49	20.6	5.5	4.1	--	8	10
50	18.9	3.3	7.5	--	2	3

FIGURE 1-

MODIFIED PILOT
VSR REACTOR

-56-

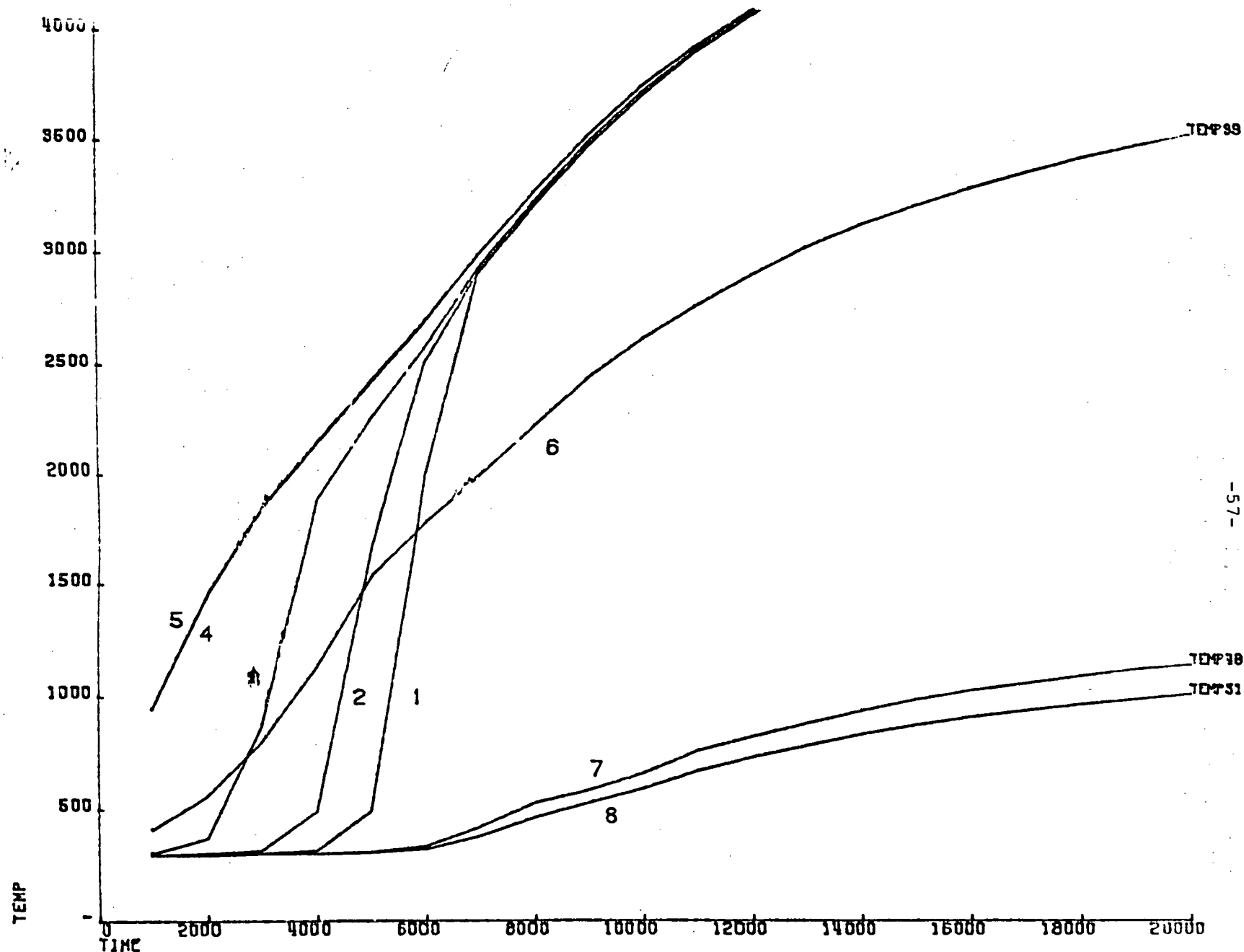
L I V U N C

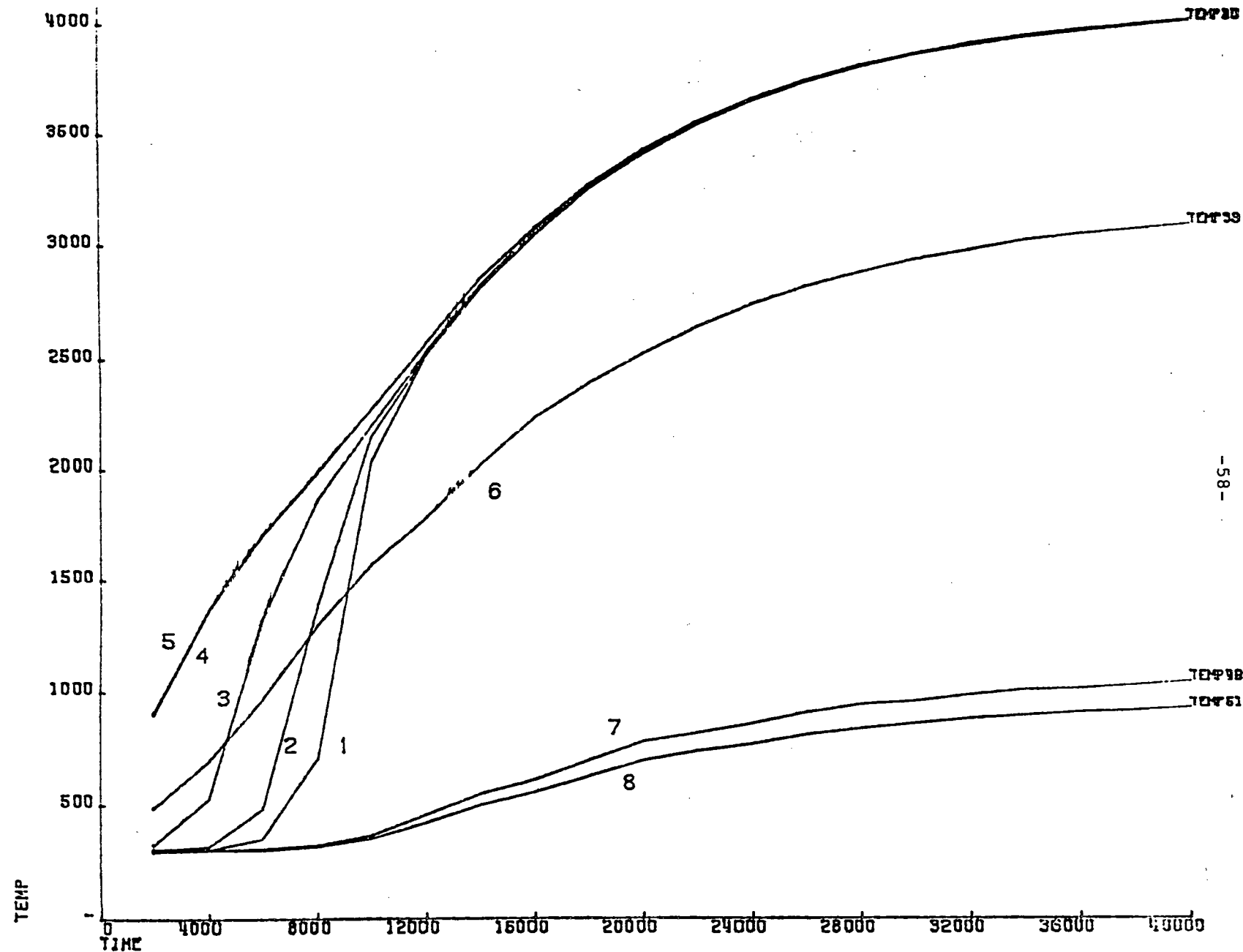


LENGTH
1 ELLER ~ 2"

WIDTH
2 ELLERS ~ 1"

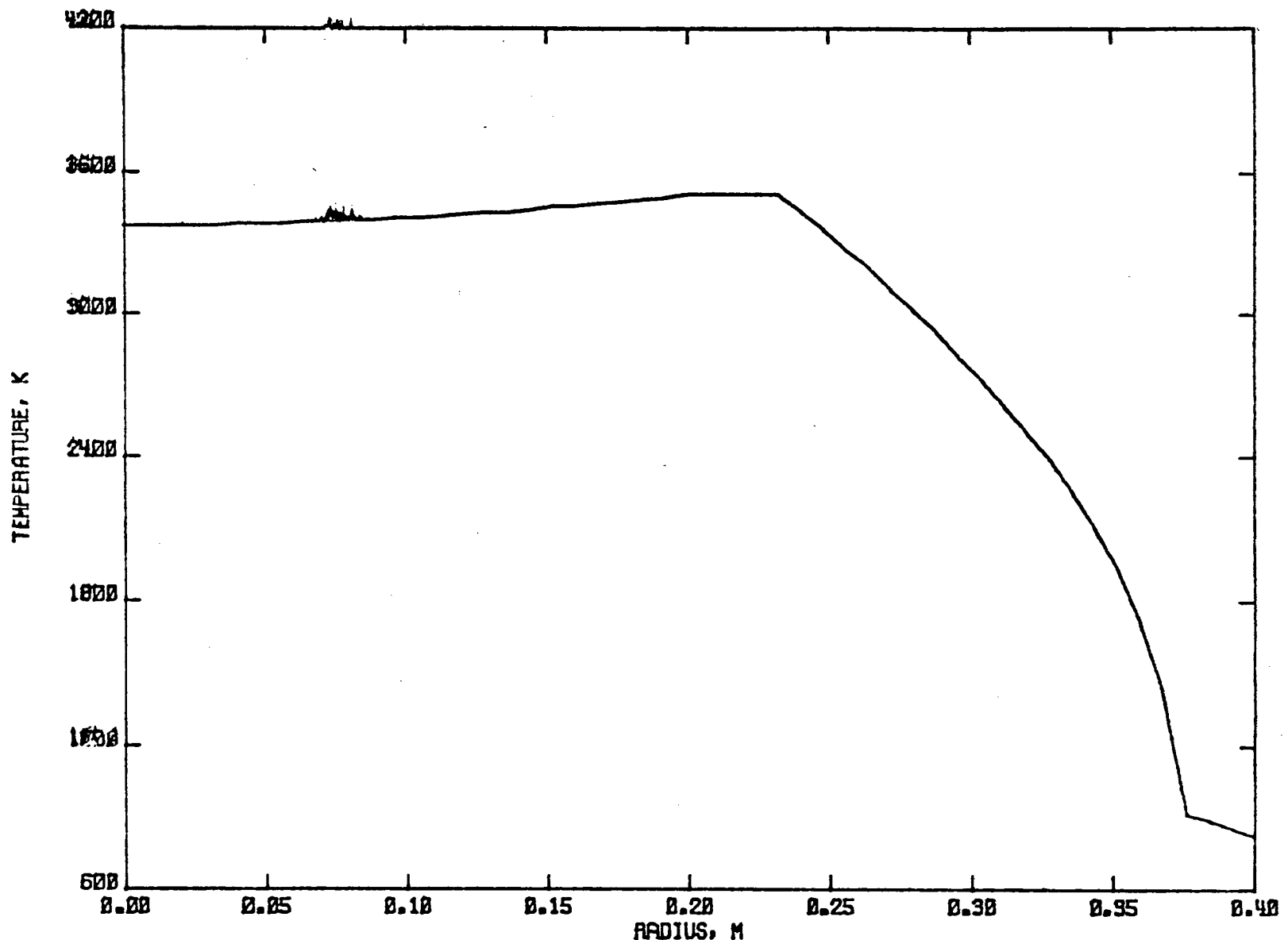
EXTERNAL
PACKED
BED





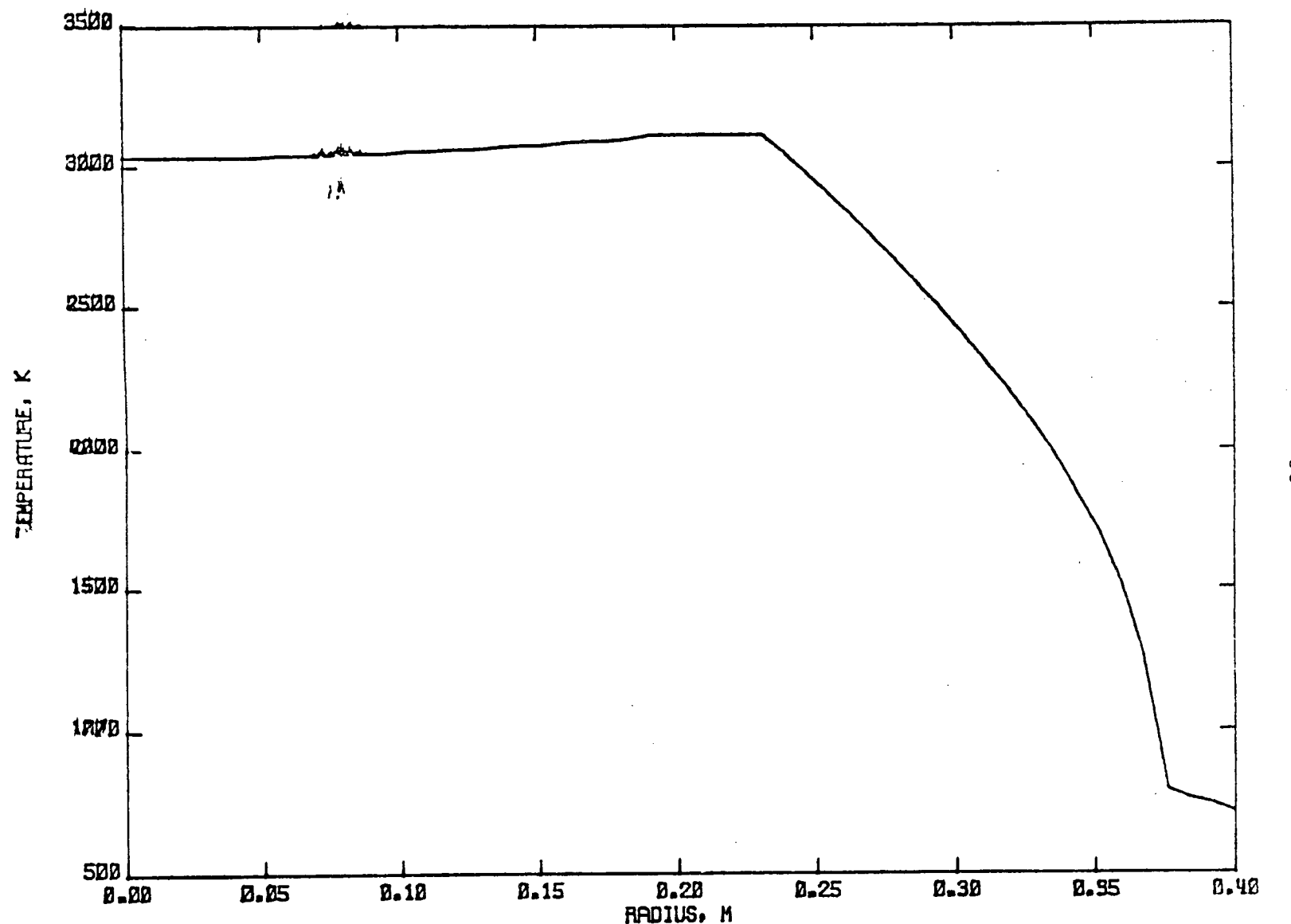
16 IN VSA RADIAL. BRICQUETTE BED. NO AXIAL HT LOSS. QUARTZ SHELL. 50 PCT. POWER

Figure 3



16-IN. VSR WITH QUARTZ SHELL STEADY-STATE TEMPERATURES VS RADIUS
BRICQUETTE BED, 100 PERCENT POWER (NOT CONVGD)

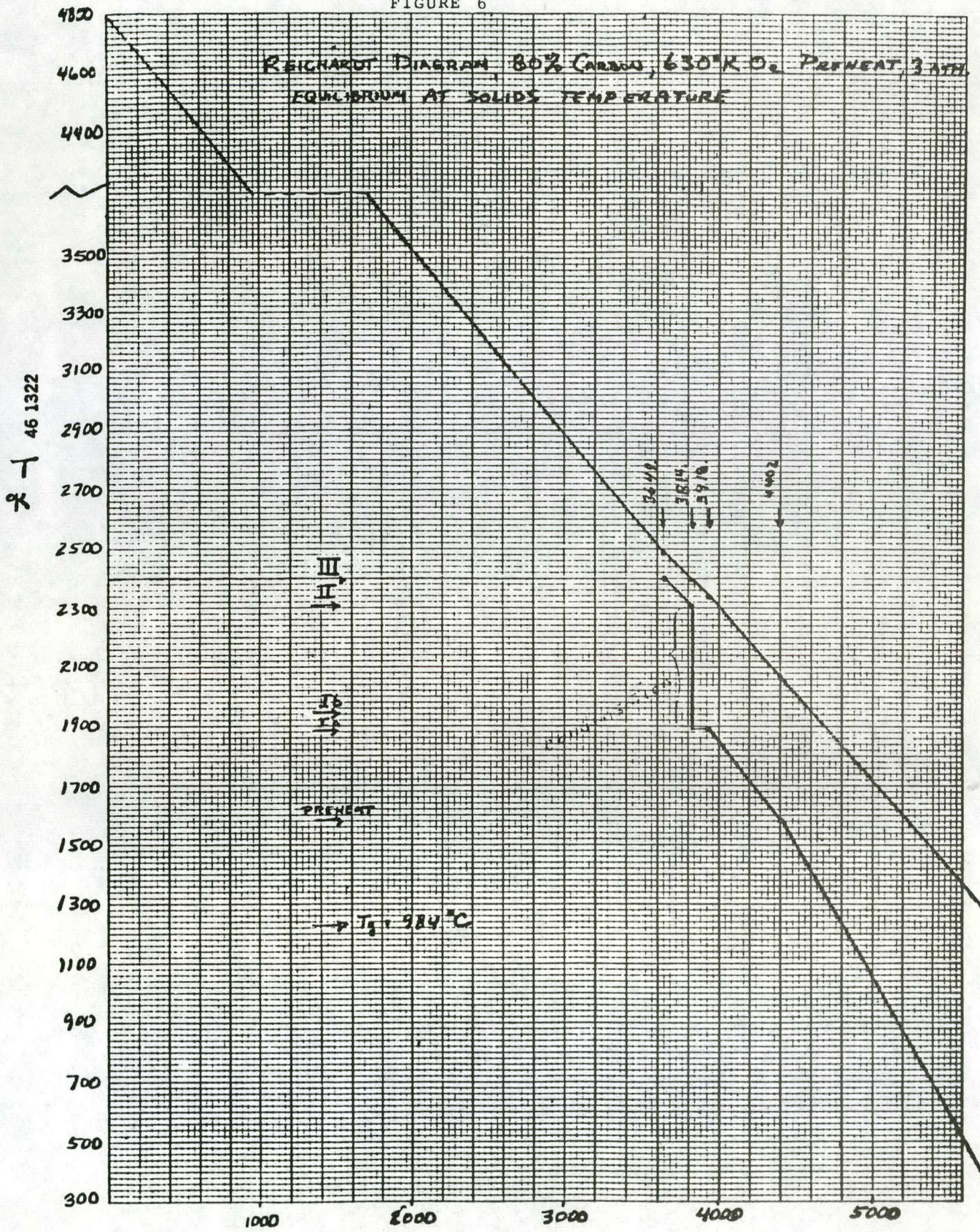
Figure 4

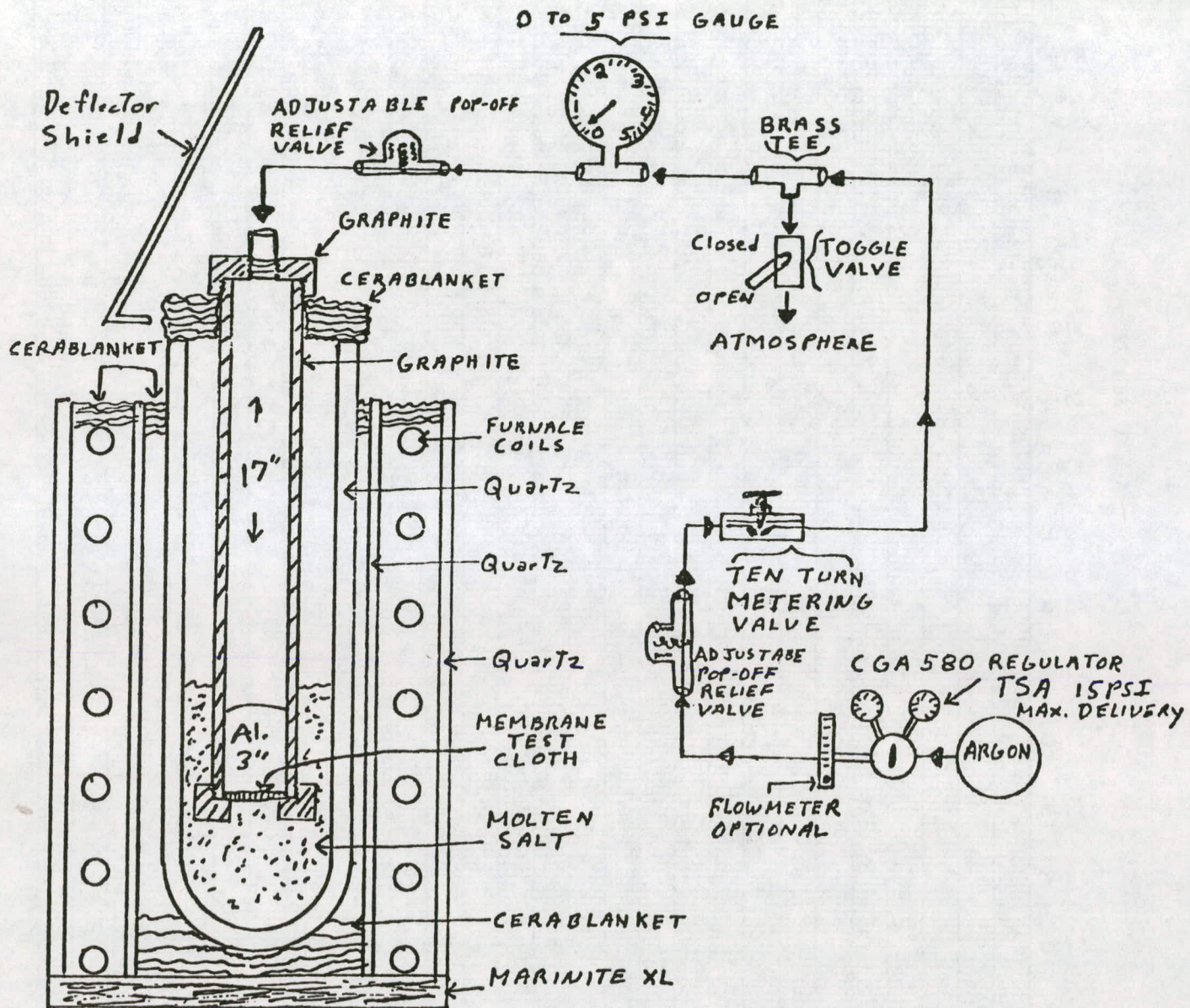


16-IN. VSR WITH QUARTZ SHELL STEADY-STATE TEMPERATURES VS RADIUS
BRICQUETTE BED, 50 PERCENT POWER

Figure 5

FIGURE 6





TEMPERATURE RANGE: 700 TO 750°C
SALT: By wt. 90% LiCl + 10% AlCl₃

PRESSURE Needed: Appx 2-3 PSI

Figure 7 Experimental Set-up for Penetration Test

UNCLASSIFIED

PRODUCTION OF ALUMINUM-SILICON ALLOY AND FERROSILICON
AND COMMERCIAL PURITY ALUMINUM BY THE
DIRECT REDUCTION PROCESS

FIRST INTERIM TECHNICAL REPORT, PHASE "C"
FOR THE PERIOD 1980 JANUARY 01 - 1980 MARCH 31

MARSHALL J. BRUNO

OCTOBER 1980

ALUMINUM COMPANY OF AMERICA
ALCOA LABORATORIES
ALCOA CENTER, PA 15069

PREPARED FOR THE
DEPARTMENT OF ENERGY
OFFICE OF THE ASSISTANT SECRETARY FOR
CONSERVATION AND SOLAR APPLICATIONS
DIVISION OF INDUSTRIAL ENERGY CONSERVATION
UNDER CONTRACT DEAC01-77CS40079

APPENDIX 1
FLWEQUIL AND FLWEQSEP PROGRAMS

CHAPTER 1
INTRODUCTION

Previous to the generation of the programs described in this report, a program named FLOWREAC was developed to simulate flowing chemical reactors. This program contained detailed modelling of the heat transfer and chemical reaction kinetics and used a "wavefront" solution of local differential equations in its computational technique. It was found that two problems limited the applicability of FLOWREAC. First, knowledge of chemical kinetic parameters required for program input was lacking in most cases, forcing iterative methods involving guessing relevant parameters and varying them until "reasonable" results were produced. Often, complex interactions of parameters were observed, complicating the solutions. Secondly, solutions were often difficult to obtain, further complicating the iterative parameter estimating process, since it was not possible to know whether lack of a solution was due to numerical difficulties or to asking an unanswerable question.

It was therefore felt that a simplification of FLOWREAC to consider only heat transfer and chemical equilibrium (i.e., elimination of chemical kinetics) was desirable. The two programs described in this report are the outgrowth of that effort. These programs are identical in all respects except their treatment of compositions of phases which flow in a direction opposite to the direction chosen for the integration to proceed. In the actual problems to which these programs have been applied, it has been necessary to specify non-equilibrium compositions for reverse-flowing phases at the start of the integration. The FLWEQUIL program will diverge if this is done, whereas the FLWEQSEP program will not. The reasons for this will be discussed in the next chapter. The necessity of starting with a non-equilibrium composition is related to the type of solution technique used by these programs. A complete steady-state model of the reactor (in which mass and heat balances on each element are performed separately and iterated until flows between each pair of elements match) would not necessitate use of non-equilibrium compositions. Since such a program is not yet available, however, the FLWEQSEP program was developed instead as an interim measure. The last stage of development of these programs

will be the generation of a steady-state iterative model, eliminating the "wavefront" solution technique now employed. However, these programs may prove useful even after a steady-state convergence program is available, since it is well known that stability problems can occur in large-scale steady-state convergence methods. The "wavefront" solution is most applicable to reactors in which recycle is not of importance.

The internal structure and data input of both FLWEQSEP and FLWEQUIL are very similar those used in FLOWREAC, since both equilibrium models were developed from FLOWREAC. The FLOWREAC program has been described in Division Report 7-79-22, and it will be assumed that the reader is familiar with that report in what follows. Differences between FLOWREAC and the programs described here will be stressed.

NOTE: A supplement to Report 7-79-22 is being prepared to reflect enhancements and corrections incorporated into FLOWREAC since the report was issued. Persons wishing to use or modify the FLOWREAC program should contact the author for current information.

Appendix 2

SUMMARY OF PRELIMINARY EXPERIMENTS
ON CARBOTHERMIC ALUMINA REDUCTION

The purpose of these experiments was to examine the effects of aluminum carbide (Al_4C_3) and silicon carbide (SiC) on vapor loss during carbothermic alumina reduction.

Alumina and graphite in a 1:3 molar ratio were mixed with various amounts of Al_4C_3 or SiC in open graphite crucibles. These were heated under 1 atmosphere of argon at about 800°C per hour to 1200°C, and then at 150°C per hour to 2150°C. Two other crucibles contained a $\text{Al}_2\text{O}_3/\text{Al}_4\text{C}_3$ and a $\text{Al}_2\text{O}_3/\text{SiC}$ mixture in amounts such that the Al_2O_3 -C ratio was 1:3. These were subjected to the same heating process as described above.

The results are shown in the first graph. The measure of recovery used was the ratio of the actual recovery to the theoretical recovery, i.e., the recovery which would occur if only carbon monoxide was lost to the gas phase. This measure is adequate on a relative scale, but may be deceiving on an absolute scale. For example, in a separate experiment, Al_4C_3 was heated in a graphite crucible. Ideally, no losses would occur, yet the recovery was only 57 percent. Presumably the losses were due to the aluminum vapor pressure above the crucible.

Comments on the results are most clearly made by considering three categories.

Graphite as main reductant- In these tests the total carbon to alumina ratio had a small positive effect on recovery regardless of the source of carbon. This raised the possibility that, since alumina can react with carbon through gaseous intermediates (e.g., Al_2O), these intermediates must "search" for carbon. This was tested in runs where the reductant was layered on top of the alumina. In the second graph, it is seen that with graphite as the main reductant layering had little effect, which appears counter to the "search" notion.

Al_4C_3 as main reductant- The original test in this category fell in line with the data for graphite reductant. In layering, however, a significant improvement was found. A "lid" was formed at the top of the

charge, presumably by carbide fusion or by reaction with the suboxide. A similar lid, though thinner, was observed in a Al_2O_3 -C- Al_4C_3 layered experiment; however, as noted in the previous section, no recovery improvement was found. Presumably, this latter "lid" was less effective because of less carbide being present and/or the inability of graphite to form a similar "lid". X-ray diffraction studies on this "lidded" run showed Al_4C_3 to be the only major compound present.

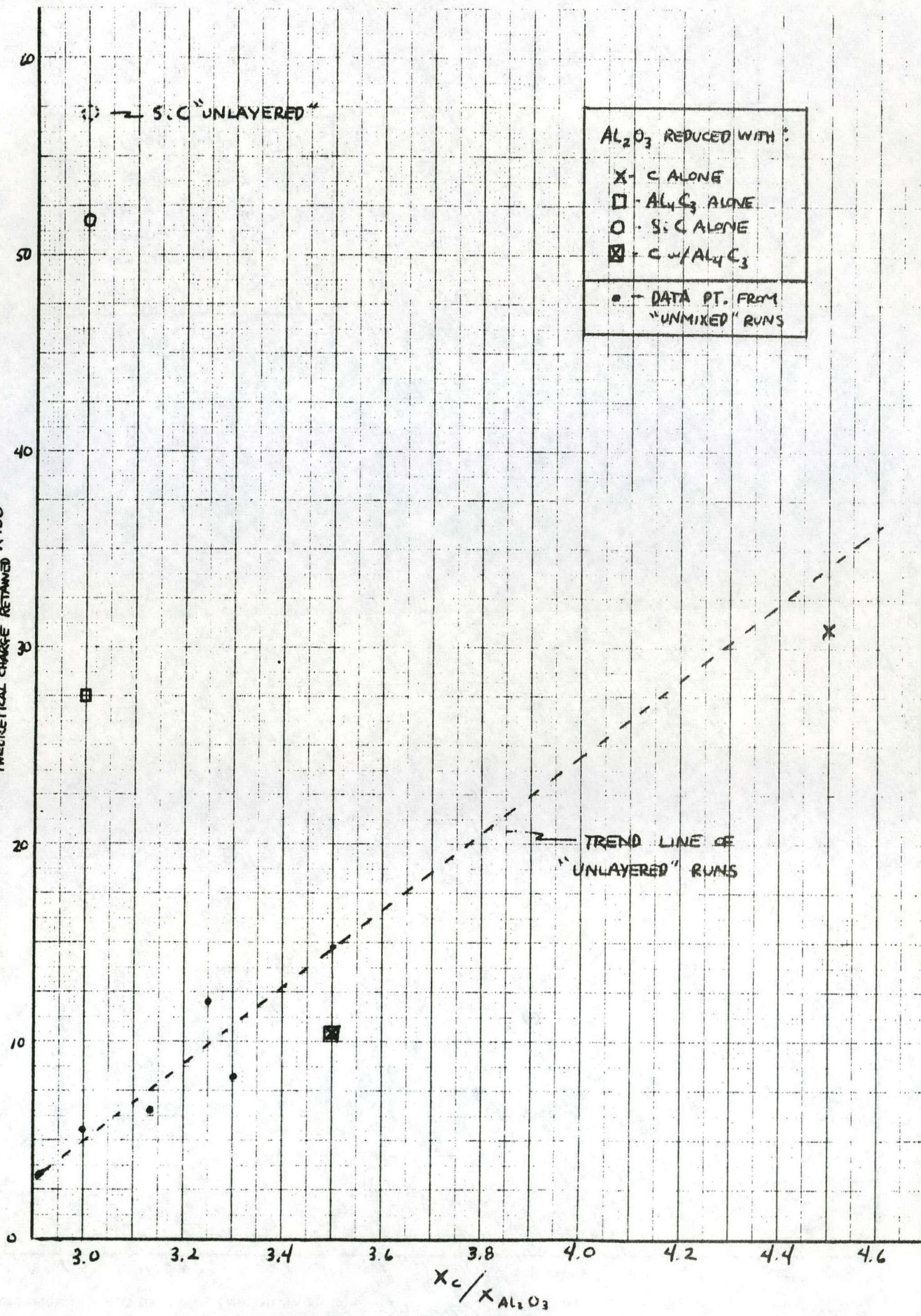
SiC as main reductant- These tests were markedly different from the first two categories. A relatively large recovery was found in the initial experiments and layering had little effect, and the recovery was on the same order as the Al_4C_3 heating experiment mentioned above. This suggested that a different type of reaction may be occurring, possibly through the lowering of aluminum vapor pressures in the various phases or by the stabilization of liquid phases with better kinetic properties. However, X-ray diffraction studies indicated that in both cases, SiC was the only compound present. Quantitative spectroscopy indicated only Si and C to be present in major amounts.

Since, in the Al-C-O ternary, OCL does not appear at less than 0.5 atmospheres of CO, these runs probably had only solid-solid reactions occurring. This could be responsible at least in part, for the non-equilibrium losses, and indicates that promoting OCL formation is crucial.

EFFECT OF CHARGE LAYERING

A-5

VERNON M-MILLAN INC. ELIZABETH, N.J. C-100
ACTUAL CHARGE RETAINED NO. 14-36111 P-247C 11/C 100 Millions to 1000 Millions • Made in U.S.A.



CHARGE RETENTION vs. C- Al_2O_3 CHARGE RATIO

A-6

